

---

Masters Theses

Student Theses and Dissertations

---

Summer 2017

## In situ pH determination based on the NMR analysis of $^1\text{H}$ -NMR signal intensities and $^{19}\text{F}$ -NMR chemical shifts

Ming Huang

Follow this and additional works at: [https://scholarsmine.mst.edu/masters\\_theses](https://scholarsmine.mst.edu/masters_theses)

 Part of the [Physical Chemistry Commons](#)

Department:

---

### Recommended Citation

Huang, Ming, "In situ pH determination based on the NMR analysis of  $^1\text{H}$ -NMR signal intensities and  $^{19}\text{F}$ -NMR chemical shifts" (2017). *Masters Theses*. 7867.  
[https://scholarsmine.mst.edu/masters\\_theses/7867](https://scholarsmine.mst.edu/masters_theses/7867)

This thesis is brought to you by Scholars' Mine, a service of the Missouri S&T Library and Learning Resources. This work is protected by U. S. Copyright Law. Unauthorized use including reproduction for redistribution requires the permission of the copyright holder. For more information, please contact [scholarsmine@mst.edu](mailto:scholarsmine@mst.edu).

***IN SITU* PH DETERMINATION BASED ON THE NMR ANALYSIS OF  
<sup>1</sup>H – NMR SIGNAL INTENSITIES AND <sup>19</sup>F – NMR CHEMICAL SHIFTS**

**by**

**MING HUANG**

**A THESIS**

**Presented to the Faculty of the Graduate School of the**

**MISSOURI UNIVERSITY OF SCIENCE AND TECHNOLOGY**

**In Partial Fulfillment of the Requirements for the Degree**

**MASTER OF SCIENCE IN CHEMISTRY**

**2017**

**Approved by:**

**Klaus Woelk, Advisor**

**V. Prakash Reddy**

**Paul Ki-souk Nam**



## ABSTRACT

The pH of an NMR sample can be measured directly by NMR experiments of signal intensities, chemical shifts, or relaxation time constants that depend on the pH. The  $^1\text{H}$  NMR peak intensities of the pH indicator phenolphthalein change as it changes from the OH-depleted form to the OH-rich form in the range of  $\text{pH} = 11.1$  to  $12.7$ . Because this range is rather small, another NMR technique was utilized based on  $^{19}\text{F}$  chemical shifts. The shift of  $\text{F}^-$  in an aqueous solution of NaF changes in the alkaline range between  $\text{pH} = 11.0$  and  $14.0$  and even more so in the acidic range between  $\text{pH} = 1.0$  and  $4.0$ . A new device made it possible for NMR samples to accurately determine pH values. The device consists of three parts: (1) an external reference (trifluoroacetic acid), (2) a temperature-sensing compound based on the chemical shifts of ethylene glycol or methanol, and (3) the pH micro-sensor compound NaF. Because pH micro-sensor compounds added to an aqueous solution have an influence on the pH, only a minimum amount of an NMR micro-sensor compound should be added to the sample. Quantitative NMR experiments in different setups (spherical NMR tubes, tubes with susceptibility plugs, Shigemi tubes) were conducted to determine the minimum amount of micro-sensor compound necessary for NMR measurements. A minimum number of  $4.02 \times 10^{16}$  nuclei was found to be sufficient for NMR signal observation using a 400-MHz spectrometer. The chemical shifts of pH-sensing NMR signals generally depend on temperature. Temperature-dependent NMR experiments were conducted to establish calibration curves through which the influence of temperature on the chemical shift can be corrected. The  $^{19}\text{F}$  signal of trifluoroacetic acid was found to have the least temperature-dependent chemical-shift variation and is suggested as independent standard for temperature-correction curves.

## ACKNOWLEDGMENTS

I would like to express my deepest gratitude to Dr. Klaus Woelk for his caring, guidance, and wisdom. Dr. Woelk's commitment to high academic standards serves as a constant source of motivation, and the environment provided to his group members could not be more conducive to excellent research. I would also like to recognize Dr. V. Prakash Reddy and Dr. Paul Ki-souk Nam for their counsel as members of my Master of Science committee. This work would also not have been possible without the support of the Missouri S&T Chemistry Department and Brewer Science Inc. of Rolla, Missouri.

I would like to express special thanks to Dr. Rex Gerald II for his continued mentorship and friendship, for his frequent assistance in the completion of experiments, and his unfaltering positive attitude no matter what difficulty I faced in the lab. His strength has carried me through the most difficult stages of this work.

I would also like to thank my mother, Jinxia Wang, my late father, Haiyu Huang, and the family of my brother, Jie Huang, for their endless love, support, and encouragement while I worked towards the completion of my dissertations. Their example has motivated me to follow a path of lifelong education, and for this (and so much more) I am forever grateful. To my other family members and friends, I would have never made it through some challenging times without your best wishes and support.

## TABLE OF CONTENTS

|  | Page |
|--|------|
| ABSTRACT.....  | iii  |
| ACKNOWLEDGEMENTS.....  | iv   |
| LIST OF ILLUSTRATIONS.....   | vii  |
| SECTION  |      |
| 1. INTRODUCTION .....  | 1    |
| 1.1.THE NEED FOR IN SITU NMR pH MEASUREMENTS.....  | 1    |
| 1.2. pH MEASUREMENTS .....   | 2    |
| 1.2.1.pH Paper.....  | 2    |
| 1.2.2. pH Electrodes .....   | 3    |
| 1.2.3. Spectroscopic in situ pH Measurements .....   | 5    |
| 1.2.3.1. pH measurement based on NMR signal intensity...5                                      |      |
| 1.2.3.2. pH measurement based on NMR chemical shift.....7                                      |      |
| 1.3. RESEARCH OBJECTIVES .....   | 11   |
| 2. METHODOLOGY .....   | 13   |
| 2.1.IN SITU NMR pH MEASUREMENT DEVICE.....   | 13   |
| 2.1.1. Standard Reference Solution.....  | 13   |
| 2.1.2. In situ NMR Temperature Measurements.....   | 18   |
| 2.1.3. pH Micro-sensor Compounds .....   | 19   |
| 2.2. NMR COIL — ACTIVE SAMPLE VOLUME.....  | 21   |
| 2.3. QUANTITATIVE NMR.....   | 21   |
| 2.3.1. Sphere NMR Tube .....   | 24   |
| 2.3.2. Doty Susceptibility Plugs.....  | 25   |
| 2.3.3. Shigemi Tube .....  | 29   |
| 2.3.4. Minimum Number of $^1\text{H}$ and $^{19}\text{F}$ Nuclei for qNMR<br>Measurements..... | 31   |
| 3. MATERIALS AND METHODS.....  | 37   |
| 3.1. MATERIALS.....  | 37   |
| 3.1.1. pH Micro-sensor Compound Based on Changes<br>in NMR Signal Intensity .....              | 37   |

|   |    |
|---|----|
| 3.1.2. pH Micro-sensor Compound Based on NMR<br>Chemical Shifts .....                   | 37 |
| 3.2. INSTRUMENTATION, KEY PARAMETERS, AND<br>PROCEDURES .....                           | 38 |
| 3.2.1. NMR Signal Acquisition and Data Processing .....                                 | 39 |
| 3.2.2. Phenolphthalein $^1\text{H}$ Experimental Procedures .....                       | 39 |
| 3.2.3. Sodium Fluoride $^{19}\text{F}$ Experimental Procedures .....                    | 39 |
| 4. RESULTS .....  | 41 |
| 4.1. IN SITU pH MEASUREMENTS IN $^1\text{H}$ NMR.....                                   | 41 |
| 4.2. IN SITU pH MEASUREMENTS IN $^{19}\text{F}$ NMR.....                                | 42 |
| 4.3. TEMPERATURE-DEPENDENT ADJUSTMENTS FOR $^{19}\text{F}$<br>NMR pH MEASUREMENTS ..... | 47 |
| 5. CONCLUSION.....  | 49 |
| BIBLIOGRAPHY.....   | 52 |
| VITA.....   | 58 |

## LIST OF ILLUSTRATION

|   | Page |
|---|------|
| Figure 1.1. Structure of the modified tripeptide Z-Ala-Pro-Phe-[2- $^{13}\text{C}$ ]-glyoxal (Z = benzyloxy-carbonyl) bonded to an enzyme (upper structure) in equilibrium with its deprotonated, anionic form (lower structure) according to ref. [2]. Numbers refer to the $^{13}\text{C}$ chemical shifts in ppm.....  | 6    |
| Figure 1.2. $^{13}\text{C}$ NMR spectra of the enzyme-bonded modified tripeptide Z-Ala-Pro-Phe-[2- $^{13}\text{C}$ ]-glyoxal (100.7 – 103.8 ppm) and its deprotonated form (107.6 – 107.8 ppm) at different pH values (from ref. [2]) .....   | 8    |
| Figure 1.3. Stacked plot of the NMR signals from the protons in meta position to each other of a mixture of 4-hydroxypyridine and cytosine at different pH values (from ref. [1] ).....   | 8    |
| Figure 2.1. $^1\text{H}$ chemical shift changes of different functional groups in deuterated chloroform ( $\text{CDCl}_3$ ). The chemical shift difference between the $\text{CH}_2$ -group signal and the OH-group signal of ethylene glycol can be used to determine the sample temperature [47]. .....   | 15   |
| Figure 2.2. $^{19}\text{F}$ chemical shift changes of pentafluorobenzene ( $\text{C}_6\text{F}_5\text{H}$ ) and sodium fluoride ( $\text{NaF}$ ) signals in aqueous solution at temperature between 300 and 325K.....   | 16   |
| Figure 2.3. The $^{19}\text{F}$ NMR chemical shift changes of sodium fluoride ( $\text{NaF}$ ) and trifluoroacetic acid ( $\text{CF}_3\text{COOH}$ ) in aqueous solution as a function of temperature between 300 and 325K.....   | 17   |
| Figure 2.4. In situ NMR pH measurement device composed of (a) 5-mm NMR tube with sample and pH micro-sensor compound, (b) 250- $\mu\text{m}$ capillary tube with chemical-shift reference compound (c) 75- $\mu\text{m}$ capillary tube with temperature-sensing compound, (d) 1-mm NMR-tube to hold the capillary tubes (b) and (c), and (e) Teflon plugs to align the 1-mm NMR tube (d) ..... | 20   |
| Figure 2.5. NMR sample tube in the magnetic radiofrequency field ( $B_1$ ) of Helmholtz saddle coils, which are typically used in superconducting NMR magnets. The $B_1$ field is homogeneous in direction and amplitude as well as perpendicular to $B_0$ in a limited volume of the sample (light orange).....  | 22   |
| Figure 2.6. Schematic of a Sphere NMR tube .....  | 24   |
| Figure 2.7. $^1\text{H}$ NMR spectrum of ethanol (4.8 Vol%) dissolved in acetone- $\text{d}_6$ in a Sphere NMR tube .....   | 26   |



|  |    |
|--|----|
| Figure 2.8. Schematics to illustrate the use of Doty susceptibility plugs in standard 5-mm NMR tubes .....   | 27 |
| Figure 2.9. $^1\text{H}$ NMR spectrum of ethanol (4.8 Vol%) dissolved in $\text{D}_2\text{O}$ (99.8% D) using Doty Aurum susceptibility plugs.....   | 28 |
| Figure 2.10. $^1\text{H}$ NMR spectrum of ethanol dissolved in a 50 Vol% $\text{D}_2\text{O}/\text{H}_2\text{O}$ solution using Doty susceptibility plugs .....  | 29 |
| Figure 2.11. Schematic of Shigemi tube. A) length of NMR tube, B) inner diameter of Shigemi NMR sample tube, B') outer diameter of tube insert, slightly smaller than B, C) length of susceptibility-matched hard glass enclosure, D) outer diameter of upper hard glass plug, a touch smaller than B.....   | 30 |
| Figure 2.12. $^1\text{H}$ NMR spectrum of a 4.8 Vol% ethanol (94%, commercial grade) $\text{D}_2\text{O}$ (99.8% D) solution in a susceptibility-matched Shigemi tube .....  | 31 |
| Figure 2.13. Setup for Shigemi tube experiments: the Shigemi tube was filled with a precisely measured 0.40 mg ethanol in 833.0 mg $\text{D}_2\text{O}$ solution, resulting in sample height of 2 mm. The sample was originally positioned in the center of Helmholtz saddle coil. In subsequent experiments, the sample volume was moved down or up from the center of coil in steps of 1 mm..... | 32 |
| Figure 2.14. Normalized integration values of the ethanol $\text{CH}_3$ -group in a 2-mm cylindrical sample height as a function of sample position, where the origin (distance = 0 mm) indicates the center of the Helmholtz saddle coils .....   | 34 |
| Figure 2.15. $^1\text{H}$ NMR spectrum obtained from a single-scan experiment of 0.1086 mL from a solution of 0.40 mg ethanol in 833.0 mg $\text{D}_2\text{O}$ in a Shigemi tube. The SNR was determined to be 130:1 .....   | 35 |
| Figure 3.1. Structural difference of the pH indicator phenolphthalein depending on the pH (ref.) .....   | 38 |
| Figure 4.1. $^1\text{H}$ NMR spectra of phenolphthalein at a) pH = 11.1. and b) pH = 12.7. Included are the two structures of phenolphthalein that are in varying equilibrium concentrations at different pH values .....  | 42 |
| Figure 4.2. Integrated $^1\text{H}$ NMR signal intensities of the OH-depleted (red data points) and OH-rich form (blue data points) of phenolphthalein as a function of pH. The black curve indicates the average ratio between red and blue data points.....  | 43 |
| Figure 4.3. $^{19}\text{F}$ chemical shift (ppm) of the pH micro-sensor compound NaF in aqueous solution as a function of pH .....   | 44 |

|   |    |
|---|----|
| Figure 4.4. $^{19}\text{F}$ NMR spectra of pentafluorododecan-3-ol and micro-sensor compound NaF in aqueous solution at two ranges of pH (acidic and basic).....  | 45 |
| Figure 4.5. $^{19}\text{F}$ NMR spectra of the pH micro-sensor compound NaF in the presence of pentafluorododecan-3-ol over the pH range from 3.58 to 4.55 .....  | 46 |
| Figure 4.6. Experimentally derived changes in the chemical shift difference between the $^{19}\text{F}$ NMR signals of NaF and trifluoroacetic acid ( $\text{CF}_3\text{COOH}$ ) at different temperatures from 300 K to 330 K..... | 48 |

## 1. INTRODUCTION

### 1.1. THE NEED FOR *IN SITU* NMR pH MEASUREMENTS

The determination of pH plays a significant role in some NMR investigations, particularly when the pH changes throughout the course of a reaction that occurs inside the NMR sample tube. Importantly, *in situ* NMR pH measurements can give insights into chemical structures, conformations, or reaction mechanisms, as well as provide information about the properties of materials for physical, chemical, and biological applications [3-5].

For example, to better understand the physicochemical processes during the hydrothermal crystallization of gels, pH values have been measured *in situ* by  $^{13}\text{C}$  NMR during the formation of SAPO-34 (silicoaluminophosphate) in the presence of hydrofluoric acid [6]. Another example of *in situ* NMR pH measurements is the determination of the extracellular pH of solid tumors in mice using  $^{19}\text{F}$  and  $^{31}\text{P}$  probes. The results provide clinical information useful for tumor diagnosis and the selection of therapies [7].

All NMR pH measurements are based on NMR-sensitive molecules for which the NMR spectrum changes along with the pH. However, it is still a challenge to use *in situ* NMR for the precise, accurate, and reasonably fast determination of pH as a function of time. On the contrary, conventional pH meters would require the removal of NMR tubes from the NMR magnet which may not be suitable for *in situ* pH measurement in fast-changing environments. It is also known that other factors influence the pH value of a test sample such as temperature, pressure, or humidity. For NMR-based *in situ* pH measurements, the chemical that is used as pH micro-sensor compound may change the

pH value in the original sample, leading to systematic measurement errors. Hence there is a need for the development of standardized *in situ* NMR pH measurement devices that offer great precision and reliability. The following section summarizes and evaluates various methods that have been used for *in situ* NMR pH measurements.

## 1.2. pH MEASUREMENTS

The abbreviation “pH” originates from a description by German scientists for the “potency of hydrogen ion concentration” (Potenz der Wasserstoffionenkonzentration). More completely, it describes the inverse of the power of  $[H^+]$ , which stands for the  $H^+$  concentration. In its mathematical definition, pH is therefore equal to the negative logarithmic value of the  $H^+$  concentration,

$$pH = -\log[H^+] \quad (1)$$

Alternatively, pH can be defined as the negative logarithmic value of the hydronium ion ( $H_3O^+$ ) concentration [1]. A hydronium ion is a hydrogen ion bonded to a water molecule, so that

$$pH = -\log[H_3O^+] \quad (2)$$

In practice, the pH of a solution is determined by measuring parameters that depend on, or that are proportional to the solution’s  $H^+$  concentration [1].

**1.2.1. pH Paper.** A simple, quick, and inexpensive approach for pH measurement in liquids is provided by using pH papers. With pH paper it is possible to measure pH to an accuracy of about  $\pm 0.2$  to  $\pm 0.5$  [8]. Accordingly, pH paper only provides a rough

estimate (order of magnitude) of the  $H^+$  concentration but rarely an exact value. Moreover, pH paper is not well-suited to reach a solution inside a typical NMR tube of 7 – 8" length.

**1.2.2. pH Electrodes.** Another common method to determine pH values is the use of pH electrodes. Those electrodes play a very important role in performing precise pH determinations and are responsible for most pH measurements in chemical experimentation and scientific publications. Among the available pH electrodes, glass electrodes are most common. In glass electrodes, differences in  $H^+$  concentrations between a standard solution inside and a sample solution outside a thin glass membrane create an electromotive force [9]. The voltage (difference in electrical potential) generated by this electromotive force is proportional to the difference in  $H^+$  concentrations and is calibrated by at least two reference buffer solution of known  $H^+$  concentrations.

Glass electrodes require substantial care and maintenance. For example, to generate an electromotive force that accurately reflects the difference in pH inside and outside of the glass membrane, the glass electrode must be kept very clean and regenerated with a reference solution after every use. Other factors such as reference junction blockages, electrolyte loss, glass bulb contaminations and the use of incorrect calibration buffers can all contribute to poor performance or calibrations curves [10, 11]. In addition, the temperature of a sample will also affect the electrode potential of a glass electrode. Hence, if there is a temperature gradient between the electrode and the sample, the pH will not be accurately determined [11].

Many different types of pH electrodes are available such as half-cell electrodes [12], specialty electrodes [13], low maintenance electrodes [14], flat-surface electrodes [15], micro and semi-micro electrodes [16], refillable epoxy electrodes [17], spear-tip electrodes [18], sure-flow electrodes [19], and triode pH electrodes [20]. It is important to consider the specific electrode features and recognize its compatibility with the sample being measured. Since not only the electrode potential but also the pH itself depends on the temperature, a triode pH electrode should be used in measurements where temperature is most critical. Triode pH electrodes make it possible to monitor sample temperatures simultaneously to electrode potentials and automatically adjust for temperature differences in a sample [21].

The pH measurement with glass electrodes is particularly challenging in very low and in very high ionic-strength samples. Special devices and calibration procedures are needed for these scenarios. For example, in high ionic-strength samples a fast-flowing, low-resistance electric junction as well as a high electrolyte salt concentration in the pH reference solution is needed [16]. It is also advisable to use a double-junction electrode in these cases, which will protect the reference electrode from salt intrusion. For best results, all calibration standards and sample temperatures should be kept within 2 °C of each other [22].

There are glass electrodes commercially available which are especially designed for pH measurement in NMR tubes. NMR tubes typically come in 3 mm, 5 mm, and 10 mm diameters, and are between 7" and 8" long. The NMR pH electrodes have their pH-sensitive glass tip mounted on a long, small-diameter rod that conveniently fits inside an NMR tube. However, these NMR pH meters come at a relatively high cost (\$400 - \$600)

[23], and the NMR tube still needs to be ejected from the NMR probe prior to the measurement. Ejecting the NMR tube for each pH measurement is not only inconvenient, but may disturb consecutive NMR measurements in a series of investigations, where the pH is supposed to be monitored simultaneously or interleaved with the NMR experiments.

**1.2.3. Spectroscopic *in situ* pH Measurements.** In addition to pH paper and pH electrodes, a pH value can also be calculated from spectroscopic data, such as UV/Vis absorbance [24], NMR signal intensities [2], or NMR chemical shifts [25, 26]. *In situ* NMR pH meters are based on specific chemicals, so-called micro-sensor compounds, that are added to the sample solution and show pH-dependent changes in signal intensities or chemical shifts.

**1.2.3.1. pH Measurement based on NMR signal intensity.** To measure pH of a sample solution by evaluating signal intensities in an NMR spectrum, the integrated intensity of at least one signal must be proportional to the number of hydrogen ions (or hydroxide ions) in the solution. An integrated intensity refers to the area under the peak and is often called “peak integral”. An unknown pH of a sample solution can be determined from a calibration of peak integrals with solutions of known pH values.

Only one report was found in the literature [2] where a reliable pH measurement based on NMR signal intensities was described. The report stated that the bio-organic compound Z-Ala-Pro-Phe-glyoxal bonded to an enzyme exists in a protonated (neutral) and a deprotonated (anionic) form (Fig. 1.1). The two forms are in pH-dependent equilibrium within the range of pH = 3.3 to 6.9 ( $pK_a \sim 5.3$ ). The equilibrium shifts in favor of the protonated form in more acidic solutions and to the deprotonated form in less

acidic solutions. This shift can be observed from the  $^{13}\text{C}$  peak integrals of the isotope-labeled Z-Ala-Pro-Phe-[2- $^{13}\text{C}$ ]-glyoxal-enzyme complex, i.e., a compound that is  $^{13}\text{C}$  labeled in the 2-carbon position of the glyoxal group (Figure 1.1). Because peak integrals are directly proportional to the number of atoms, the ratio of the peak integrals directly reflect the ratio of the protonated to deprotonated form. Outside this range, only one of the two forms (protonated for  $\text{pH} < 3.3$ , or deprotonated for  $\text{pH} > 6.9$ ) exists in sufficient concentration, and only the signal of this one form is observed.

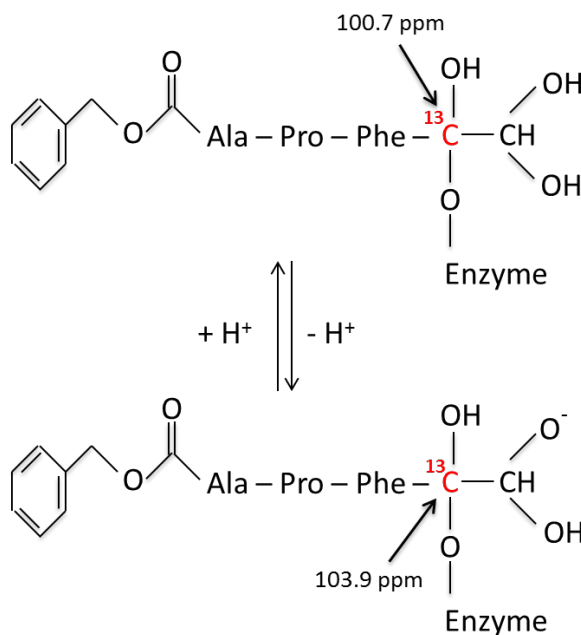


Figure 1.1. Structure of the modified tripeptide Z-Ala-Pro-Phe-[2- $^{13}\text{C}$ ]-glyoxal (Z = benzyloxy-carbonyl) bonded to an enzyme (upper structure) in equilibrium with its deprotonated, anionic form (lower structure) according to ref. [2]. Numbers refer to the  $^{13}\text{C}$  chemical shifts in ppm.

Outside the range of  $\text{pH} = 3.3$  to  $6.9$ , the signals of only one form of the Z-Ala-Pro-Phe-[2- $^{13}\text{C}$ ]-glyoxal-enzyme compound is observed ( $\text{pH} > 6.9$ , deprotonated form;  $\text{pH} < 3.3$ , protonated form) and the  $^{13}\text{C}$  peak integrals don't change with  $\text{pH}$ . Within the



range of pH = 3.3 to 6.9, the peak integral of the protonated, isotope-labeled form ( $\delta = 100.7$  ppm) decreases with increasing pH while the peak integral of the deprotonated form ( $\delta = 107.8$  ppm) increases (Figure 1.2).

It is noted that, in addition to the peak integral, the chemical shifts in this example also change. The change is more pronounced for the protonated form where the  $^{13}\text{C}$  signal shifts from  $\delta = 100.7$  ppm (at pH = 3.3) to  $\delta = 103.8$  ppm (at pH = 6.9); it is less pronounced in the deprotonated form where it only shifts from  $\delta = 107.6$  ppm to  $\delta = 107.8$  ppm as the pH changes from 3.3 to 6.9. It is further noted that the  $^{13}\text{C}$  isotope-labeled signals become broader in the middle of the pH-sensitive range (pH  $\sim 4$  to 5). The fact that the  $^{13}\text{C}$  isotope-labeled signals become broader and that the signals shift toward each other in the pH-sensitive range is an additional indication for the dynamics of an equilibrium where the NMR signals broaden because of a limited lifetime of the exchanging partners, i.e., the protonated and deprotonated species.

**1.2.3.2.pH measurement based on NMR chemical shift.** To measure pH of a sample solution by evaluating chemical shifts in an NMR spectrum [27], the position of a resonance signal must change depending on the pH of the solution. Many literature reports are available where a reliable pH measurement based on NMR chemical shifts is described. For example, the chemical shifts of the protons in the meta position to each other of 4-hydroxypyridine and cytosine in a mixture of the two compounds change considerably within the range of pH = 9.5 to pH = 13.5 (Figure 1.3) [1]. Outside this range, the NMR chemical shift does not change.

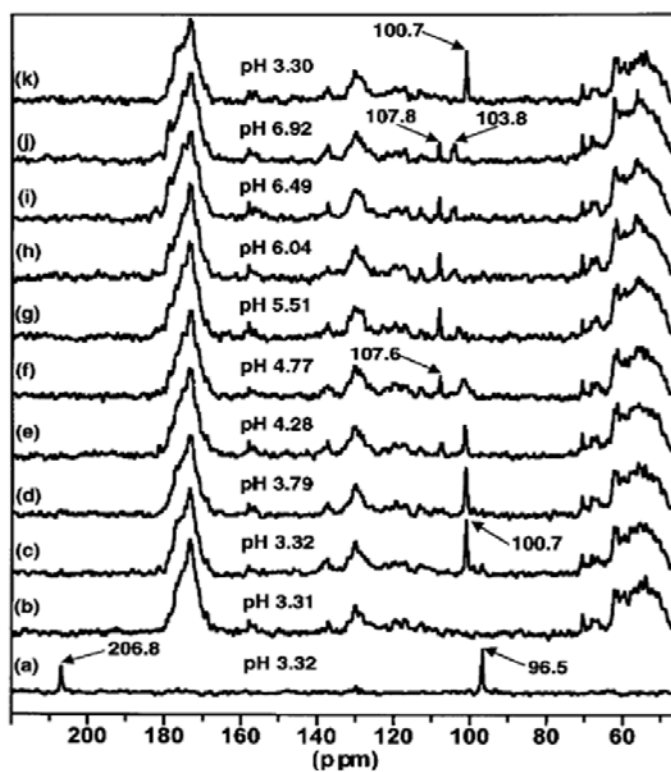


Figure 1.2.  $^{13}\text{C}$  NMR spectra of the enzyme-bonded modified tripeptide Z-Ala-Pro-Phe-[2- $^{13}\text{C}$ ]-glyoxal (100.7 – 103.8 ppm) and its deprotonated form (107.6 – 107.8 ppm) at different pH values (from ref. [2]).

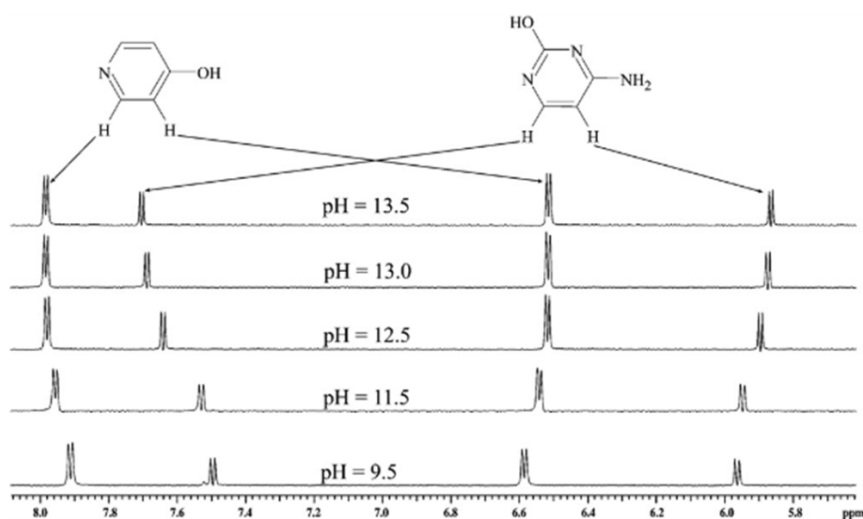


Figure 1.3. Stacked plot of the NMR signals from the protons in meta position to each other of a mixture of 4-hydroxypyridine and cytosine at different pH values (from ref. [1]).

Because many NMR signals shift in their resonance frequency (even though the shift may be small) with changing environments and reaction conditions, a pH dependency of a chemical shifts must be measured against a standard for which the chemical shift is not affected by a changing pH [28, 29]. Alternatively, if the pH-dependency of a compound's chemical shift is known, a calibration curve of pH versus chemical shift can be used to accurately predict the pH of an unknown solution.

In many cases, it has been suggested to add specific pH-sensitive chemicals (NMR pH micro-sensor compounds) to a solution [30] for which the chemical shift dependency on pH is known. In  $^1\text{H}$  NMR spectroscopy, examples of such chemicals are acetic acid ( $\text{CH}_3\text{CO}_2\text{H}$ ), chloroacetic acid ( $\text{CH}_2\text{ClCO}_2\text{H}$ ) or dichloroacetic acid ( $\text{CHCl}_2\text{CO}_2\text{H}$ ) for pH  $\sim 0$  to 4 [31], formic acid ( $\text{HCO}_2\text{H}$ ) or sodium formate ( $\text{HCO}_2\text{Na}$ ) for pH  $\sim 0$  to 5 [32], and TRISH $^+$  (tris(hydroxymethyl)aminomethane ( $\text{CH}_2\text{OH}$ ) $_3\text{CNH}^+$ ) for pH  $\sim 5$  to 10 [33].

Chemical-shift-dependent NMR measurements of pH values may not only be conducted with proton NMR but also with NMR of other nuclei such as  $^{13}\text{C}$ ,  $^{15}\text{N}$ ,  $^{19}\text{F}$ , or  $^{31}\text{P}$ . Essentially, any NMR-sensitive nucleus that is in close proximity to a pH-sensitive proton of a weak acid or weak base can function as an “indirect” pH micro-sensor [34]. For example, sodium malate, sodium citrate, and the dipeptide carnosine were shown to be effective  $^{13}\text{C}$  NMR micro-sensor compounds for different pH ranges [35]. Furthermore,  $^{13}\text{C}$  signals of sodium carbonate, sodium bicarbonate, or dissolved carbon dioxide were used to measure pH values from 9 to 12 [36, 37]. The amino acid histidine has been used in  $^{15}\text{N}$  spectroscopy to provide information about pH in the range from 6 to 9.7 [38]. Inorganic phosphate is the most commonly used pH micro-sensor in  $^{31}\text{P}$  NMR

[39], which has also been used to measure pH in biological cells [40]. Other known  $^{31}\text{P}$ -NMR micro-sensors are glucose-6-phosphate, other sugar phosphates [41], or [N-(P,P-dimethylphosphinoylmethyl)-N-(P-hydroxy-P-methylphosphinoylmethyl)amino] methylphosphonic acid [31]. The latter is particularly interesting because it can be used for a rather large range of pH from 0 to 12. The chemical shift of inorganic fluoride was used with  $^{19}\text{F}$  NMR spectroscopy to determine renal tubular cellular pH values from pH ~ 5.6 to 8.0 [42]. Fluorine compounds are particularly interesting as NMR micro-sensors because  $^{19}\text{F}$  spectroscopy is often used to provide direct, non-invasive measurements of the metabolism of fluorinated drugs such as those used in cancer treatments [43]. A series of nontoxic, fluorinated amino acids and their methyl esters have been used to measure intracellular pH in human peripheral blood lymphocytes by  $^{19}\text{F}$  NMR [44]. Monofluoromethylaniline and trifluoromethylaniline show a single resonance in  $^{19}\text{F}$  NMR which can be used to measure pH values from 6 to 9.7 [45]. Other fluorinated anilines and p-fluoroanilines were used as micro-sensors for pH values from 0 to 1 [44]. While these aniline compounds take time to adjust to an external pH value,  $^{19}\text{F}$  spectroscopy with plain fluoride ions ( $\text{F}^-$ ) is known to give rapid results in the range of pH from 1.5 to 4.5 [46].

In conclusion, NMR micro-sensors used to measure pH values *in situ* in an NMR tube while recording NMR spectra are based on specific chemicals that are added to the sample solution showing pH-dependent changes in signal intensities or chemical shifts. There are several advantages of using such *in situ* NMR micro-sensors: (a) there is no need to eject a sample tube from the NMR magnet for the pH measurement, (b) the pH measurement can be recorded as spectral imprimatur, i.e., in the same spectrum that is

used for structural analysis, (c) it is convenient to determine the pH values from peaks recorded in an NMR spectrum that is automatically saved in the sample's data file, and (d) the pH of a solution can be recorded during the course of a reaction conducted and monitored *in situ* in the NMR magnet.

Finally, however, it must be mentioned that the temperature of a solution plays an important role for the pH and its measurements. In NMR, the temperature has not only an influence on the pH, but often also on the chemical shift of the micro-sensor and sometimes even on the range of pH that is accessible through NMR. For example,  $^{13}\text{C}$  spectroscopy with morpholine as micro-sensor was used to measure pH values from 5.5 to 7.3 at room temperature [6], while the range of 7.3 to 10.3 was accessible at 120 °C [6].

### 1.3. RESEARCH OBJECTIVES

The main objective of this thesis is to develop a protocol for an accurate *in situ* NMR pH measurement that utilizes the spectra of small and quantifiable amount of pH micro-sensor compounds. The micro-sensor compounds used for *in situ* NMR analysis must change their chemical shift or signal intensities depending on the pH of the solution so that the pH may be determined according to a calibration curve. Specific objectives include:

- 1) Development of an *in situ* NMR pH measurement device that utilizes micro-sensor compounds in the test sample solution.
- 2) Including an independent external reference for absolute calibration of the NMR chemical shift in the device.

3) Including a known external temperature-sensing NMR reference to adjust for temperature-dependent chemical-shift changes

4) Utilizing detailed quantitative NMR to calculate the minimum amount of micro-sensor compound needed for in situ NMR pH measurement, thus minimizing the effect of the micro-sensor compound on the pH of the solution.

## 2. METHODOLOGY

### 2.1. *IN SITU* NMR pH MEASUREMENT DEVICE

The *in situ* NMR pH measurement device developed in this thesis consists of three parts. The first part is a standard reference solution which provides an absolute chemical-shift reference for the *in situ* NMR pH measurements. The reference solution is intended to satisfy two criteria: (1) the chemical shift should be constant under changing pH conditions and (2) the chemical shift should be constant under changing temperatures. The second part of the NMR pH meter is a compound that can be used to determine the temperature of the NMR sample *in situ*. This is usually accomplished by measuring a temperature-dependent chemical-shift difference between two peaks of the same compound. [47] The third part is the actual pH micro-sensor compound.

Due to the inherent insensitivity of NMR signals, a rather sizeable amount of pH detector molecules is generally necessary to acquire NMR signals with a sufficient single-to-noise ratio. However, a large amount of detector molecules can significantly influence the pH of a sample solution. Therefore, to ensure accurate measurement of the pH, an NMR-sensitive pH detector molecule must be considered which can be used in very small and quantifiable amounts. The following sections explain in detail the compounds and components that were used in this work to construct a highly sensitive and accurate *in situ* NMR pH meter.

**2.1.1. Standard Reference Solution.** As mentioned before, *in situ* NMR pH measurement devices are based on specific chemicals (pH micro-sensor compounds) that are added to the sample solution showing pH-dependent changes in signal intensities or chemical shifts (Section 1.2.3.1 and 1.2.3.2). When signal intensities are used to

determine pH values, a quantitative standard (qNMR standard) is needed to calibrate the signal intensities, and a chemical-shift standard is needed when the pH is measured based on differences in chemical shifts. The reference intensities or chemical-shift standards should be independent of the sample pH. This can be accomplished by using an external reference that is not in contact but measured together with the sample solution. In this work, a capillary tube (250  $\mu\text{m}$  i.d., 360  $\mu\text{m}$  o.d.) filled with a reference material was always inserted concentrically into standard 5-mm NMR sample tubes to provide an external reference.

Another important feature for the reference solution is that the signal intensities or the chemical shifts, respectively, must be insensitive to temperature. For example, literature and independent measurements show that the  $^1\text{H}$  chemical shift of the  $\text{CH}_3$ -group of methanol or the  $\text{CH}_2$ -group of ethylene glycol are less dependent on temperature ( $< 3.0 \times 10^{-3}$  ppm/K, Figure 2.1) while the OH-group signals of methanol or ethylene glycol are very temperature sensitive ( $> 7.9 \times 10^{-3}$  ppm/K) [50]. The reason for this dependency is that the extent of hydrogen bonding among the OH-groups is temperature dependent. At higher temperatures there is less extensive hydrogen bonding resulting in a higher electron density around the OH-groups. Changing electronic orbital angular momentums and electron density contributions from excited vibrational and rotational states at higher temperature may also contribute to variations in chemical shifts. The higher electron density leads to an increased shielding of the OH proton and an upfield shift of the OH resonance in the direction of the aliphatic  $\text{CH}_3$  and  $\text{CH}_2$  signals. Because of the temperature sensitivity of the  $^1\text{H}$  resonances of the OH-group and the relative stability of the  $^1\text{H}$  resonances of the  $\text{CH}_2$ -groups and  $\text{CH}_3$ -groups, methanol and ethylene



glycol have been used as standards for chemical shift calibration and, simultaneously, to determine the temperature of the sample (see Section 2.1.2).

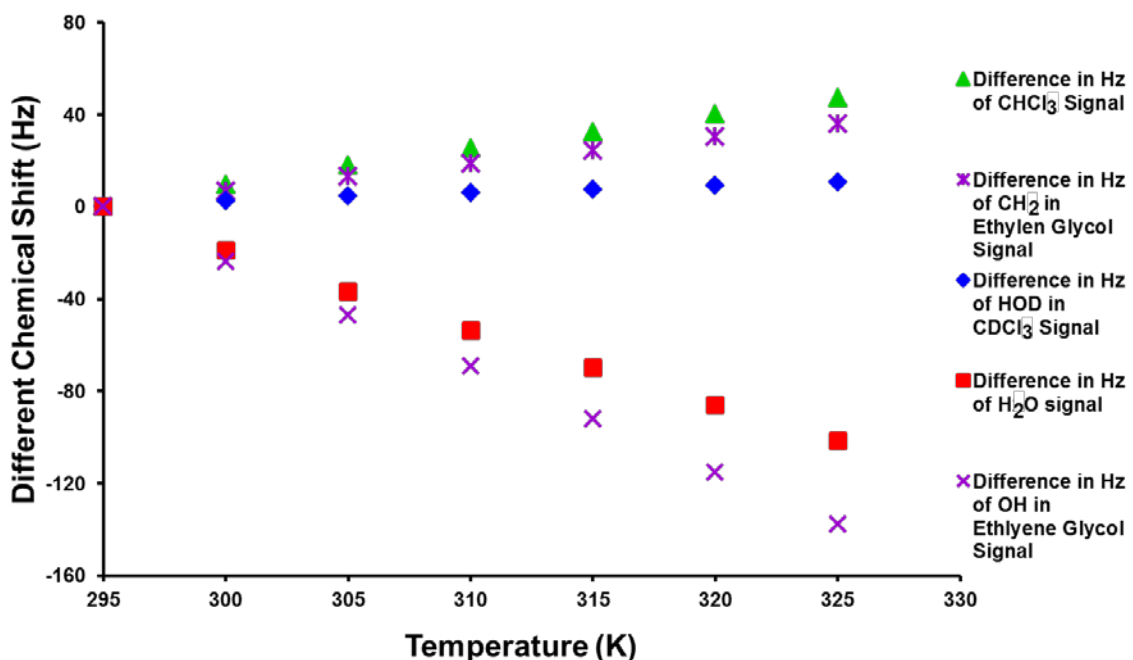


Figure 2.1.  $^1\text{H}$  chemical shift changes of different functional groups in deuterated chloroform ( $\text{CDCl}_3$ ). The chemical shift difference between the  $\text{CH}_2$ -group signal and the OH-group signal of ethylene glycol can be used to determine the sample temperature [50].

In an attempt to find the chemical shift of a functional group that exhibits a very small temperature dependence,  $^1\text{H}$  NMR experiment were performed with solutions of ethylene glycol dissolved in deuterated chloroform ( $\text{CDCl}_3$ ) at various temperatures. As evident from Figure 2.1, the chemical-shift change of the ethylene glycol  $\text{CH}_2$  groups with temperature is relatively small ( $2.997 \times 10^{-3}$  ppm/K); however, the change in chemical shift of the HOD signal is even smaller ( $0.875 \times 10^{-3}$  ppm/K). HOD is formed

by partial deuteration of H<sub>2</sub>O molecules due to an exchange of hydrogen with deuterium atoms from the CDCl<sub>3</sub> solvent molecules. Because the slope of the chemical shift vs. temperature is smallest for the HOD signal, HOD could be used as preferred reference signal for NMR measurements such as the *in situ* pH determination studied here.

For <sup>19</sup>F NMR spectroscopy, it is rather difficult to find chemical compounds with an NMR signature that is nearly independent of temperature. For example, even in the gas phase where molecules are considered most independent of external influences, <sup>19</sup>F chemical shifts of the compounds CF<sub>3</sub>CF<sub>3</sub>, CF<sub>3</sub>Br, CF<sub>3</sub>Cl, and CHF<sub>3</sub> change noticeably ( $> 1.80 \times 10^{-3}$  ppm/K) when the temperature is raised from 260 to 360 K [47]. Moreover, as determined experimentally and shown in Figure 2.2, the <sup>19</sup>F chemical shifts of pentafluorobenzene (C<sub>6</sub>F<sub>5</sub>H) and sodium fluoride (NaF) in aqueous solution change drastically ( $22.5 \times 10^{-3}$  ppm/K and  $56.8 \times 10^{-3}$  ppm/K, respectively) when the temperature is raised by only 25 K from 300 to 325 K.

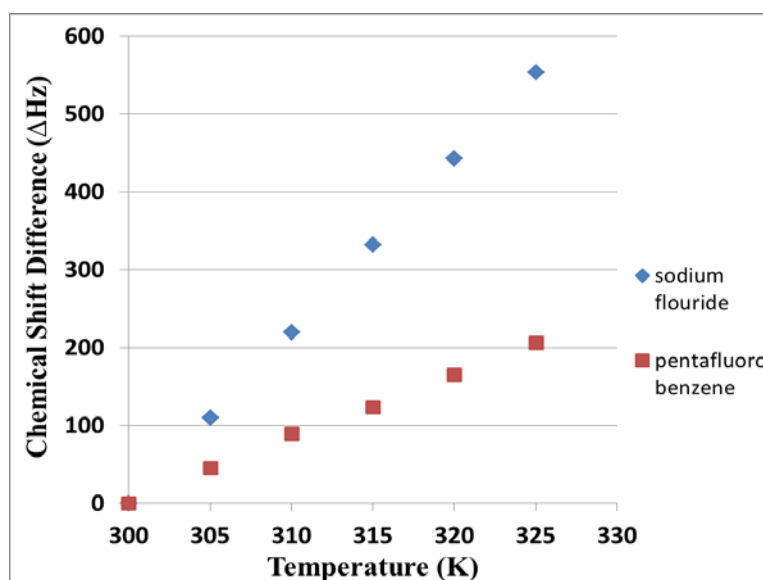


Figure 2.2. <sup>19</sup>F chemical shift changes of pentafluorobenzene (C<sub>6</sub>F<sub>5</sub>H) and sodium fluoride (NaF) signals in aqueous solution at temperature between 300 and 325 K.

During the investigations of this work it was found that the  $^{19}\text{F}$  signal of trifluoroacetic acid ( $\text{CF}_3\text{COOH}$ ) has a comparably small dependency on temperature. Figure 2.3 shows the  $^{19}\text{F}$  chemical-shift changes of NaF and  $\text{CF}_3\text{COOH}$  as a function of temperature between 300 and 325 K. While the  $^{19}\text{F}$  chemical shift of NaF changes by  $56.8 \times 10^{-3}$  ppm/K, the  $\text{CF}_3\text{COOH}$   $^{19}\text{F}$  signal changes by only  $2.54 \times 10^{-3}$  ppm/K. This is the smallest change of chemical shift as a function of temperature known thus far in solution  $^{19}\text{F}$  NMR spectroscopy. Only fluorine compounds in the gas phase are known to show an even smaller chemical shift dependency on temperature.

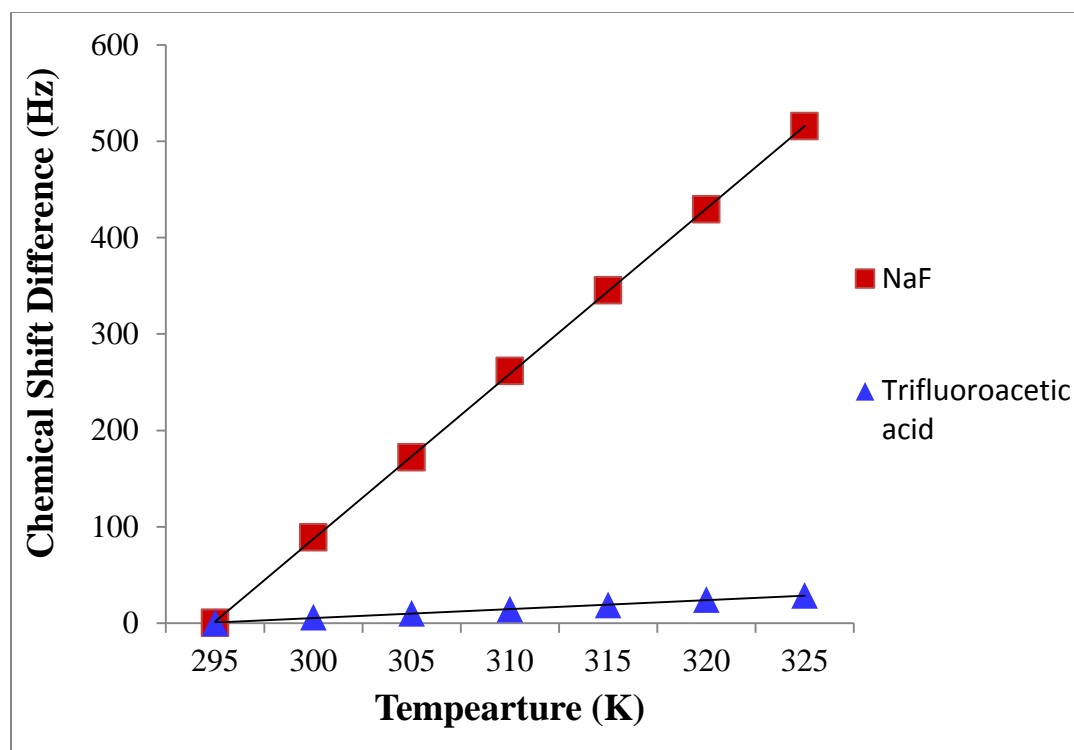


Figure 2.3. The  $^{19}\text{F}$  NMR chemical shift change of sodium fluoride (NaF) and trifluoroacetic acid ( $\text{CF}_3\text{COOH}$ ) in aqueous solution as a function of temperature between 300 and 325 K.

It is noted that the  $2.54 \times 10^{-3}$  ppm/K chemical shift change for the  $\text{CF}_3$  signal in trifluoroacetic acid ( $\text{CF}_3\text{COOH}$ ) is equivalent to a  $0.31 \times 10^{-3}$  % relative shift in a  $^{19}\text{F}$  NMR spectrum, which typically spans 800 ppm (367.3 Hz equals 1 ppm in a 400 MHz NMR spectrum) while the  $0.875 \times 10^{-3}$  ppm/K chemical shift change of HOD in  $\text{CDCl}_3$  is equivalent to a  $7.29 \times 10^{-3}$  % in a typical 12 ppm  $^1\text{H}$  NMR spectrum (400 Hz equal 1 ppm in a 400 MHz NMR spectrum). The chemical shifts in both cases, HOD for  $^1\text{H}$  spectroscopy and  $\text{CF}_3\text{COOH}$  for  $^{19}\text{F}$  spectroscopy, may be considered insensitive to temperature and can most often be neglected. As such, HOD in  $\text{CDCl}_3$  is a good chemical-shift reference for *in situ*  $^1\text{H}$  NMR pH measurements while neat trifluoroacetic acid is a good chemical-shift reference for  $^{19}\text{F}$  NMR pH measurements.

**2.1.2. *In situ* NMR Temperature Measurements.** Methanol and ethylene glycol have been used as NMR thermometer [48-50], i.e., as temperature-sensing compounds in  $^1\text{H}$  NMR spectroscopy. Temperature sensing molecules in NMR spectroscopy must have a chemical shift difference between two signals that changes with temperature according to a known functionality. While this functionality may be preferred to be linear, any such relationship between the chemical shifts of two functional groups and the sample temperature can be determined from a temperature calibration curve. For example, Methanol is known as temperature sensing molecule for sample temperatures between 178 and 330 K [50]. The calibration relationship is:

$$T[\text{K}] = 409.0 - 36.54 \Delta\delta - 21.85 (\Delta\delta)^2 \quad (3)$$

where  $\Delta\delta$  is the chemical shift difference between the two functional groups in ppm.

Ethylene glycol is another well-known temperature-sensing compound that can be used at sample temperatures between 273 and 416 K. The corresponding equation to

calculate temperature shows a linear relationship [50] according to:

$$T[K] = 466.5 - 102.00 \Delta\delta \quad (4)$$

**2.1.3. pH Micro-sensor Compounds.** *In situ* NMR pH measurements are based on specific chemicals, so-called micro-sensor compounds, that are added to the sample solution and that show pH-dependent changes in signal intensities or chemical shifts. To ensure the least interference of the pH micro-sensor compound with the pH of the solution and thus warrant an accurate measurement of the sample pH, highly NMR-sensitive pH micro-sensor compounds should be considered that can be used in very small amounts. An investigation was conducted to determine the minimal amount of micro-sensor compound that is needed to observe  $^1\text{H}$  and  $^{19}\text{F}$  NMR spectra without a significant influence on the pH of the sample solution.

The investigation consisted of three steps: a) special NMR tubes were used to determine the absolute concentration of the pH micro-sensor compound, b) experiments were designed to determine the range of strong and homogeneous radiofrequency field ( $B_1$  field) in the active sample volume, and c) the minimum number of nuclei needed for NMR pH measurements in  $^1\text{H}$  and  $^{19}\text{F}$  experiments was determined. From the minimum number of nuclei, it should generally be possible to calculate the influence of the micro-sensor compound on the pH of the sample considering the acid/conjugated base equilibrium of the micro-sensor compound and the quantity of the sample tested.

Figure 2.4 shows the newly developed *in situ* NMR pH measuring device consisting of: (a) a 5-mm NMR tube filled with the NMR sample solution and the pH micro-sensor compound, (b) a capillary tube (250- $\mu\text{m}$  i.d. 350- $\mu\text{m}$  o.d.) filled with

trifluoroacetic acid as chemical-shift reference, (c) a capillary tube (75- $\mu\text{m}$  i.d. 150- $\mu\text{m}$  o.d.) filled with ethylene glycol or methanol as a temperature-sensing compound. As shown in Fig. 2.3, the small capillary tube (c) is placed inside the larger capillary tube (b). They are both mounted inside a separate 1-mm tube (d) that is then placed inside the 5-mm NMR tube (a).

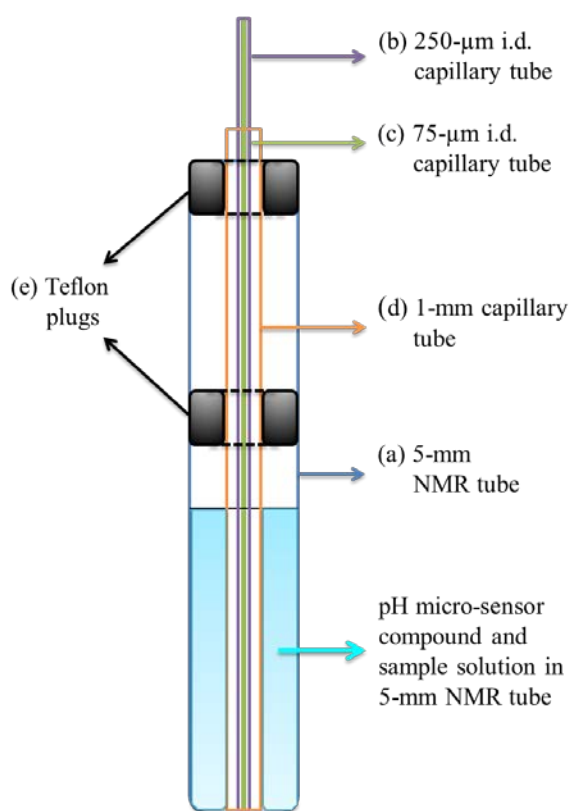


Figure 2.4. *In situ* NMR pH measurement device composed of (a) 5-mm NMR tube with sample and pH micro-sensor compound, (b) 250- $\mu\text{m}$  capillary tube with chemical-shift reference compound (c) 75- $\mu\text{m}$  capillary tube with temperature-sensing compound, (d) 1-mm NMR-tube to hold the capillary tubes (b) and (c), and (e) Teflon plugs to align the 1-mm NMR tube (d).

This assembly is preferred because the 1-mm NMR tube (d) can easily be placed concentrically along the long axis of the 5-mm NMR tube (a) using commercially

available Teflon plugs (e). It was found that the 75- $\mu$ m capillary tube sample volume (c) is sufficient for observing the resonances of ethylene glycol and methanol in  $^1\text{H}$  NMR spectra acquired with typical parameters. Trifluoroacetic acid, however, requires a larger capillary tube sample volume to be observed in both  $^1\text{H}$  and  $^{19}\text{F}$  NMR spectra.

## 2.2. NMR COIL- ACTIVE SAMPLE VOLUME

Figure 2.5 shows schematically how an NMR sample tube is positioned inside the Helmholtz saddle coil of a typical superconducting NMR magnet. The coil is part of a tuned circuit that delivers the radiofrequency (RF) pulses to the sample and detects the RF response from the sample.

RF fields delivered by and detected from the coil must ideally be perpendicular to the static magnetic field ( $B_0$ ) for maximum NMR sensitivity. The most efficient way to deliver and detect RF fields is to use horizontally mounted solenoid coils. However, horizontal coils would require the probe to be removed from the magnet when samples are exchanged. A less efficient but more convenient assembly is the vertical Helmholtz saddle coil as shown in Figure 2.4. The Helmholtz saddle coil generates a region of nearly strong and homogeneous magnetic field perpendicular to  $B_0$ , which allows NMR sample tubes to be conveniently inserted into and ejected from the probe with a pneumatic system [9, 51].

## 2.3. QUANTITATIVE NMR

Quantitative NMR (qNMR) refers to the use of NMR spectroscopy to determine absolute amounts and concentrations of one or more chemical species in solution [52].

Conducting qNMR properly to a very high precision takes some special considerations. In one-dimensional single-pulse NMR spectroscopy without hyperpolarization or polarization transfer from or to other nuclei, the area under an NMR peak is directly proportional to the number of NMR-active nuclei in the sample. The sample concentration can therefore be deducted by comparison to signals from compounds of known concentrations. Because the NMR response is equal for all nuclei of the same type

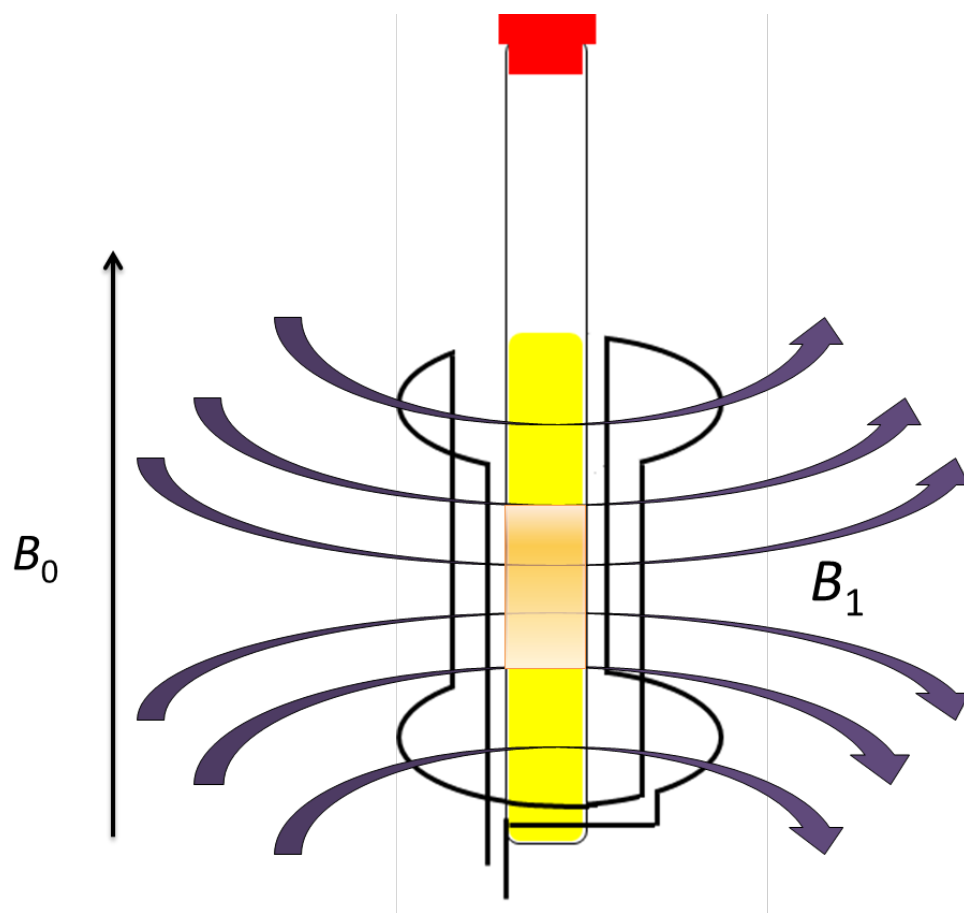


Figure 2.5: NMR sample tube in the magnetic radiofrequency field ( $B_1$ ) of Helmholtz saddle coils, which are typically used in superconducting NMR magnets. The  $B_1$  field is homogeneous in direction and amplitude as well as perpendicular to  $B_0$  in a limited volume of the sample (light orange).



(e.g.,  $^1\text{H}$ ), qNMR is a superior technique for quantifying amounts and concentrations, while other techniques may suffer from compound-specific response factors [53]. Unlike other spectroscopic techniques such as UV/Vis absorbance spectroscopy, qNMR usually doesn't require elaborate sample preparation or compound separation. In addition, qNMR offers its uniquely rich structural information together with the quantitative information. It is therefore not surprising that qNMR has found its place in several fields of research and routine analytical measurements as a basic technique. These fields include determination of the purity of pharmaceutical drug ingredients [54, 55], quantification of natural products [56] or pharmaceutical compounds [57], forensic analyses [58], food sciences [59], and the test for purity of organic molecules in chemical synthesis [60]. In this study, qNMR was used to determine the minimum amount of micro-sensor compound that must be dissolved in a sample volume to accurately measure the pH *in situ* with NMR spectroscopy. To define this minimum amount, it is important to understand the NMR response from the inhomogeneous  $B_1$  field of the Helmholtz saddle coil. In several series of experiments utilizing different but well-defined sample geometries, the extent of the  $B_1$  field in the center of the Helmholtz saddle coil was measured. A concentration standard that is placed in the strong and homogeneous central area of the  $B_1$  field will then make it possible to determine the absolute number of nuclei ( $^1\text{H}$  or  $^{19}\text{F}$ ) necessary to generate an NMR signal with sufficient SNR.

In this study, different types of specialty NMR tubes (i.e., Sphere (ref.) tubes, tubes utilizing Doty (ref.) susceptibility plugs, and Shigemi (ref.) tubes) were used to confine the sample volume to a very small volume. This volume can then be moved along

the direction of the main magnetic field  $B_0$  (z axis) in order to measure the NMR response and determine the extent of the strongest and most homogeneous  $B_1$  field.

**2.3.1. Sphere NMR Tube.** Figure 2.6 shows the so-called Sphere NMR tube of the Wilmad-Lab Glass Company. It has a 18- $\mu$ L spherical sample container at the bottom of the tube, which is the only part that is intended to be filled with sample solution [61]. This way, it creates a spherical sample volume which is largely independent of the magnetic susceptibility of surrounding materials.

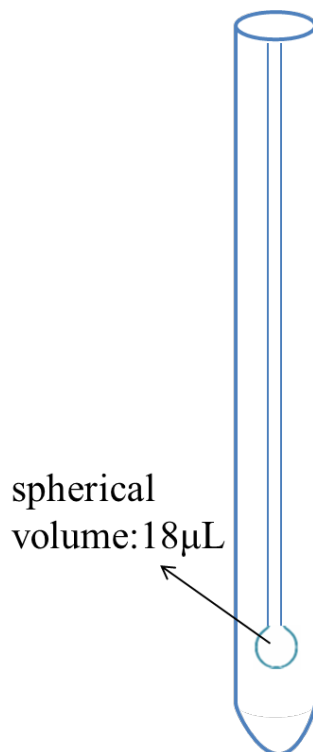


Figure 2.6. Schematic of a Sphere NMR tube

A solution was prepared by adding 5  $\mu$ L of ethanol (94%, commercial grade) to 100  $\mu$ L of deuterated acetone (acetone- $d_6$ , 95%, not purified). 18  $\mu$ L of this solution was

added into the spherical part of a Sphere NMR tube and analyzed with  $^1\text{H}$  NMR. Figure 2.7 shows the NMR spectrum from the ethanol/acetone- $\text{d}_6$  solution (4.8 Vol%) consisting of four NMR signals. They are assigned to the  $\text{CH}_3$  and  $\text{CH}_2$  groups of ethanol, the remaining protons of acetone- $\text{d}_6$ , and a combined signal consisting of  $\text{H}_2\text{O}$  protons and ethanol OH protons. However, the  $\text{CH}_3$  and  $\text{CH}_2$  groups are expected to be observed as triplet and quartet signals, respectively. Remaining susceptibility mismatches between the sample solution and the spherical sample container, however, led to a low resolution NMR spectrum where it was impossible to resolve the triplet and quartet signals. The low resolution of the NMR spectrum influenced the accuracy of the qNMR measurements, particularly with respect to integration of NMR signals that are in close proximity to other signals. Additional issues arose from filling the sample into the spherical sample volume, which always led to material being deposited along the capillary portion of the Sphere NMR tube. The sample was typically filled with a capillary tube that was small enough to fit inside the Sphere NMR capillary. However, it was unavoidable that the filling capillary touched the inner surface of the Sphere NMR capillary, leaving some material on the inner wall of the Sphere NMR capillary. This material contributes to the NMR signal, which prevented obtaining an accurate relationship between NMR signal intensities and the absolute numbers of nuclei in the sample.

**2.3.2. Doty Susceptibility Plugs.** A NMR tube utilizing so-called susceptibility plugs manufactured by Doty Scientific is shown in Figure 2.8. These susceptibility plugs are provided as sets of two plugs together with a positioning rod and collar. The upper face of both plugs has a threaded hole that lets you firmly attach the positioning rod. While the lower plug is positioned at the bottom of the NMR tube, the upper plug is held

at a desired position in the tube above a sample volume by the positioning rod. To stabilize the upper plug position, the rod is held by a collar that rests on top of the tube [62].

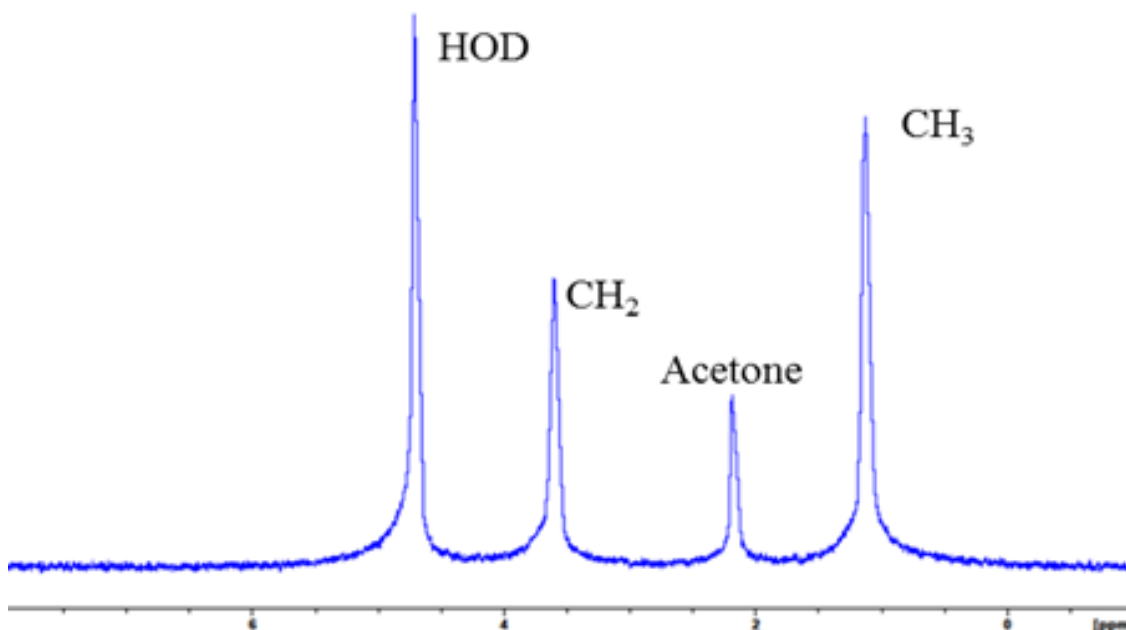


Figure 2.7.  $^1\text{H}$  NMR spectrum of ethanol (4.8 Vol%) dissolved in acetone- $\text{d}_6$  in a spherical NMR tube.

Traditionally, sample sizes are 3-5 times the height of the central area of the NMR probe's RF coil. With the use of Doty susceptibility plugs, magnetic field distortions from susceptibility discontinuities that typically occur at the interface between the upper air and the sample as well as the interface between the lower glass and the sample are far removed from the sample. With this assembly, the sample is placed only in the area of strong and homogeneous  $B_1$  field. [63]

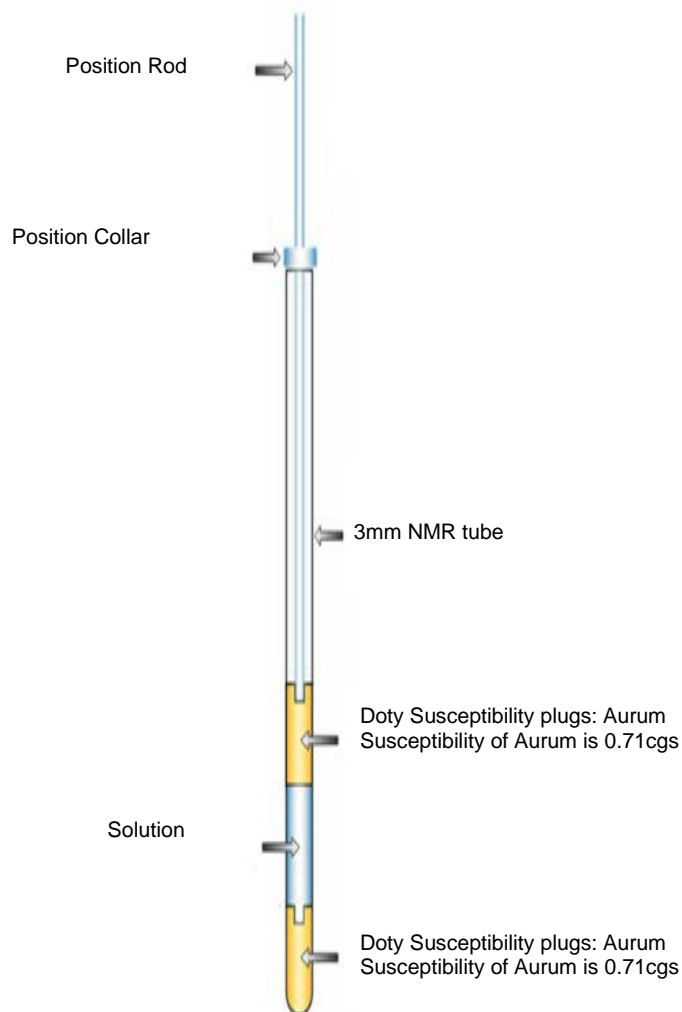


Figure 2.8. Schematic s to illustrate the use of Doty susceptibility plugs in standard 5-mm NMR tubes

In this study, Doty susceptibility Aurum plugs matched to the susceptibility of  $D_2O$  were used. The  $^1H$  NMR spectrum of 5  $\mu l$  ethanol (94%, commercial grade) in 100  $\mu l$   $D_2O$  (99.8% D) is shown in Figure 2.9. The baseline of the spectrum is not flat, which influences the accuracy of signal integration. Similar to the Sphere NMR tube investigation, the triplet and quartet peaks of the  $CH_3$  or  $CH_2$  group are poorly resolved.

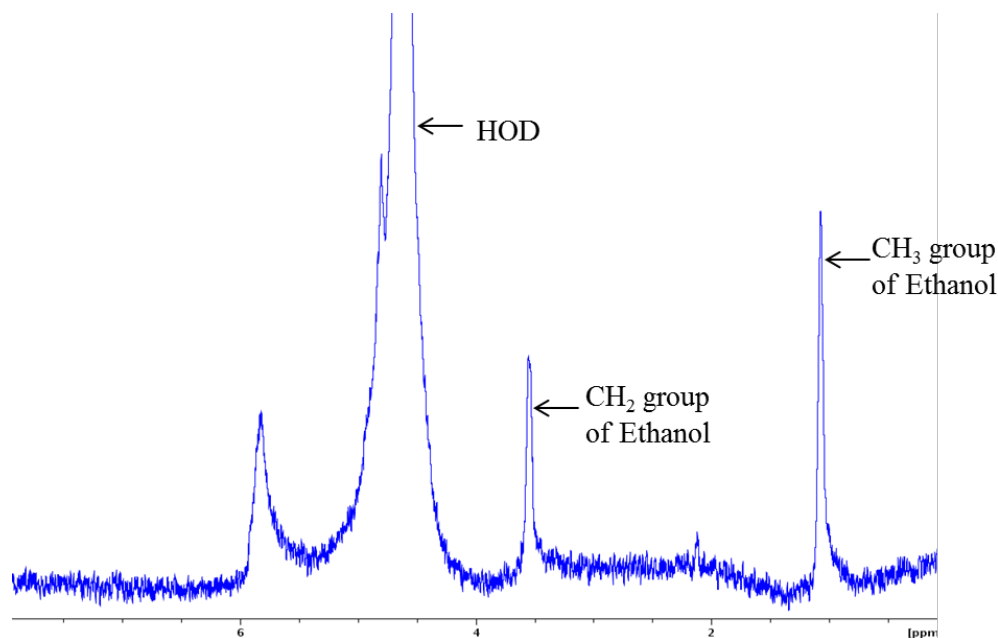


Figure 2.9.  $^1\text{H}$  NMR spectrum of ethanol (4.8 Vol%) dissolved in  $\text{D}_2\text{O}$  (99.8% D) using Doty Aurum susceptibility plugs.

The susceptibility of the Doty Aurum plugs is listed as  $\kappa = 0.71$  (in cgs units); while the susceptibility of  $\text{D}_2\text{O}$  is reported as  $\kappa = 0.70$ . It appears that the small susceptibility difference of  $\Delta\kappa = 0.01$  is sufficient to substantially distort the magnetic field homogeneity, so that a resolution of the ethanol triplet and quartet is no longer possible. To better match susceptibilities, a 1:1 mixture of  $\text{H}_2\text{O}$  ( $\kappa = 0.72$ ) and  $\text{D}_2\text{O}$  ( $\kappa = 0.70$ ) was used as the solvent resulting in exactly the desired volume susceptibility of  $\kappa = 0.71$ . Figure 2.10 shows the spectrum of a sample composed of 50 Vol%  $\text{D}_2\text{O}$  and  $\text{H}_2\text{O}$  with  $5\mu\text{L}$  of ethanol. A flat baseline is observed in the NMR spectrum, and the triplet and quartet signals of ethanol are well resolved.

However, another issue was found that renders the Doty susceptibility plugs unsuited for accurate determination of the minimum amount of nuclei needed for *in situ* pH NMR measurements. The bottom plug in the Doty assembly is not snugly attached

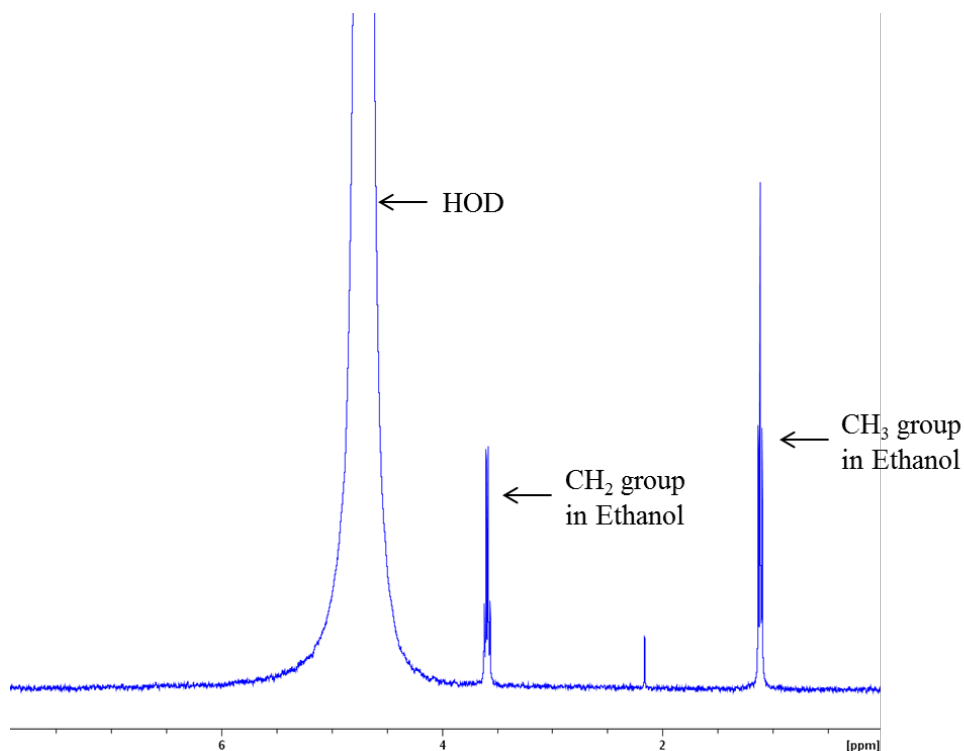


Figure 2.10.  $^1\text{H}$  NMR spectrum of ethanol dissolved in a 50 Vol%  $\text{D}_2\text{O}/\text{H}_2\text{O}$  solution using Doty susceptibility plugs.

to the bottom of the NMR tube and a gap remains between the glass wall and the plug. Some of the sample solution will creep between the bottom plug and the glass wall, which will interfere with accurately determining the absolute number of nuclei in the intended sample region.

**2.3.3. Shigemi Tube.** Figure 2.11 shows a so-called Shigemi tube manufactured by Shigemi Inc. They are made from a special type of chemically inert hard glass and can be purchased as matched to the magnetic susceptibility of different standard solvents. Accordingly, different solvents require different tubes. A Shigemi tube consists of an outer NMR tube (5 mm o.d.) and a tube insert (4.1 mm o.d.) that fits snugly into the outer tube. [64]

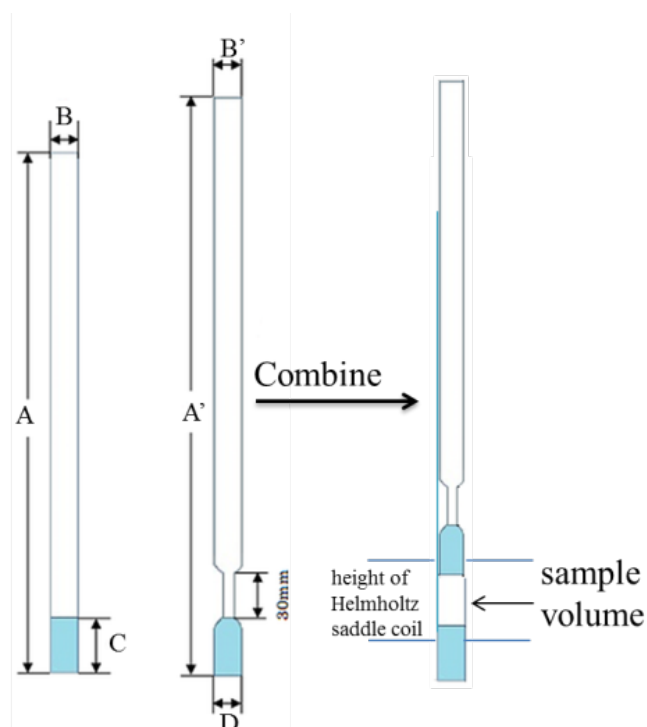


Figure 2.11. Schematic of Shigemi tube. A) length of NMR tube, B) inner diameter of Shigemi NMR sample tube, B') outer diameter of tube insert, slightly smaller than B, C) length of susceptibility-matched hard glass enclosure, D) outer diameter of upper hard glass plug, a touch smaller than B.

Figure 2.12 shows a high-resolution  $^1\text{H}$  NMR spectrum of a solution prepared by dissolving 5  $\mu\text{L}$  of ethanol (94%, commercial grade) in 100  $\mu\text{L}$   $\text{D}_2\text{O}$  (99.8% D). The sample is completely and exclusively contained in the sample area of the Shigemi tube, i.e., the sample is placed between of the susceptibility-matched hard-glass parts of the Shigemi tube. The NMR spectrum exhibits a flat baseline and well-resolved  $J$ -couplings of the ethanol's  $\text{CH}_2$  quartet and  $\text{CH}_3$  triplet. Because the lower hard-glass area is permanently fused with the NMR tube, no material can creep below the intended sample volume. As a result, the Shigemi tube delivers the best results for the qNMR applications in this work.



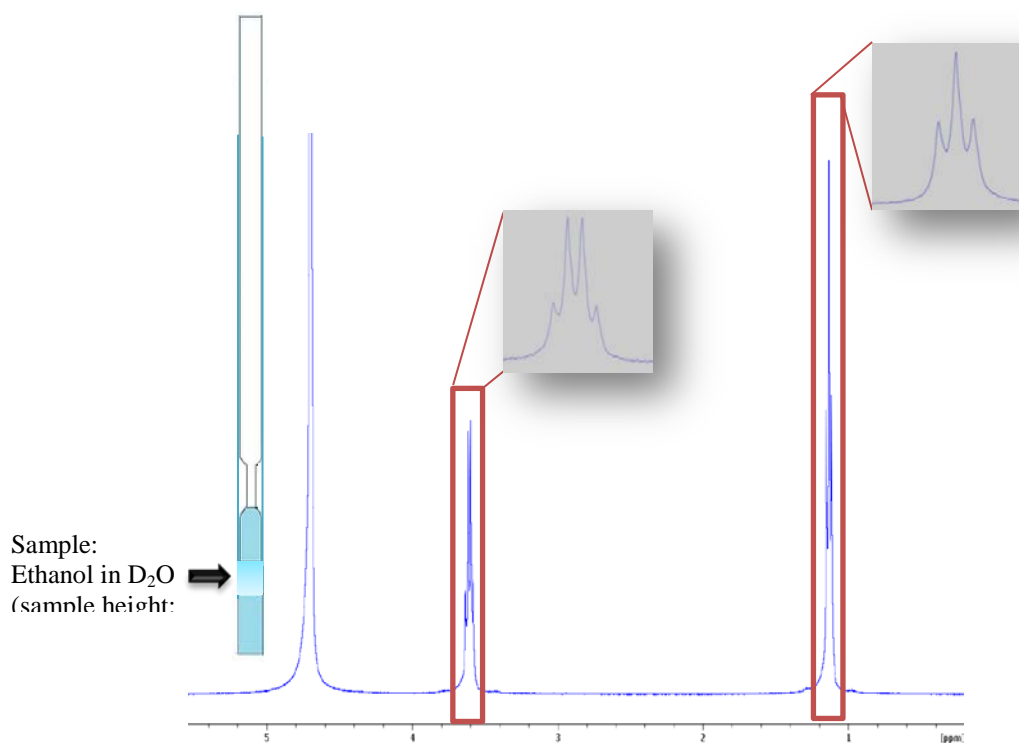


Figure 2.12.  $^1\text{H}$  NMR spectrum of a 4.8 Vol% ethanol (94%, commercial grade) D<sub>2</sub>O (99.8% D) solution in a susceptibility-matched Shigemi tube.

#### 2.3.4. Minimum Number of $^1\text{H}$ and $^{19}\text{F}$ Nuclei for qNMR Measurements.

From the discussion of the different types of specialty NMR tubes (Sections 2.3.1 – 2.3.3), the Shigemi tube was found to perform best for a determination of the minimum number of NMR-active nuclei (e.g., protons in  $^1\text{H}$  NMR). In addition, the Shigemi tube sample volume can easily be positioned in the center of the strong and homogeneous  $B_1$  field of the NMR probe.

A series of NMR experiments was conducted to determine the region of the strong and homogenous  $B_1$  field. Figure 2.13 shows the principal setup for these experiments, which were executed as follows: a) 0.40 mg ethanol was dissolved in

833.0 mg D<sub>2</sub>O leading to 0.796 mL solution. b) 0.1086 mL of this solution was placed between the hard-glass upper plug and the fixed hard-glass bottom of the Shigemi tube leading to a 2.0-mm cylindrical sample height, c) the Shigemi tube was positioned in the NMR probe such that the sample volume is placed in the center of the probe's Helmholtz saddle coils, d) a <sup>1</sup>H-NMR spectrum was recorded. e) the sample volume was moved in steps of 1 mm down from the center of the coil and another NMR spectrum recorded. f) step e) was repeated until the sample reached 16 mm below the center of the coil, g) the sample was re-positioned in the coils' center, and again, a NMR spectrum was recorded, h) steps e) and f) were repeated but this time by moving the sample up in steps of 1 mm until the sample reached 16 mm above the coils' center.

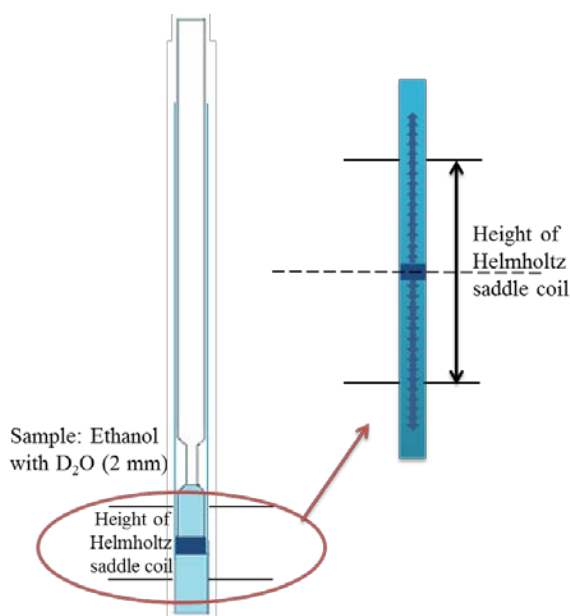


Figure 2.13. Setup for Shigemi tube experiments: the Shigemi tube was filled with a precisely measured 0.40 mg ethanol in 833.0 mg D<sub>2</sub>O solution, resulting in sample height of 2 mm. The sample was originally positioned in the center of Helmholtz saddle coil. In subsequent experiments, the sample area was moved down or up from the center of coil in steps of 1 mm.

In the end, thirty two NMR spectra were recorded. The ethanol CH<sub>3</sub>-group signal was integrated in each spectrum and the maximum integral normalized to 100. It is noted that qNMR typically uses an absolute integral (i.e., not a normalized integral) obtained from a homogenous  $B_1$  field to quantify the number of chemical compounds of interest. Figure 2.14 shows the result of the normalized integration values in percent of the ethanol CH<sub>3</sub>-group as a function of sample volume position. It shows that more than 99% of the maximum normalized integral value is obtained from a volume that stretches about 6 mm about the coils' center, i.e., 3 mm above and 3 mm below the coils' center. Similarly, more than 90% of the maximum integral value is obtained from a volume that stretches 12 mm about the coils' center. The 6-mm range (3 mm above and 3 mm below the center) was chosen in this study to determine the minimal amount of micro-sensor compound that is needed to reasonably observe <sup>1</sup>H and <sup>19</sup>F NMR spectra but minimizing the influence on the pH of the sample solution. The 6-mm range was also selected so that the entire sample experienced uniform excitation and reception sensitivity.

The volume of a standard 5-mm NMR sample tube (4.8 mm i.d.) that falls within the 6-mm range of strong and homogeneous  $B_1$  field was calculated to be 0.1086 mL. Because 0.40 mg of ethanol was used in the original solution (0.733 mL) but only 0.1086 mL of this solution was used in this experiment, the total number of ethanol molecules in the 2.0-mm sample volume is  $7.15 \times 10^{17}$ . Hence the number of molecules in the 6-mm inner coil volume is  $2.15 \times 10^{18}$  ( $= 3 \cdot 7.15 \times 10^{17}$ ). Figure 2.15 shows a high-resolution <sup>1</sup>H NMR spectrum of the ethanol solution in the Shigemi tube obtained in a single scan. The signal intensity of the CH<sub>3</sub> group shows a SNR (signal-to-noise ratio) of 130:1.

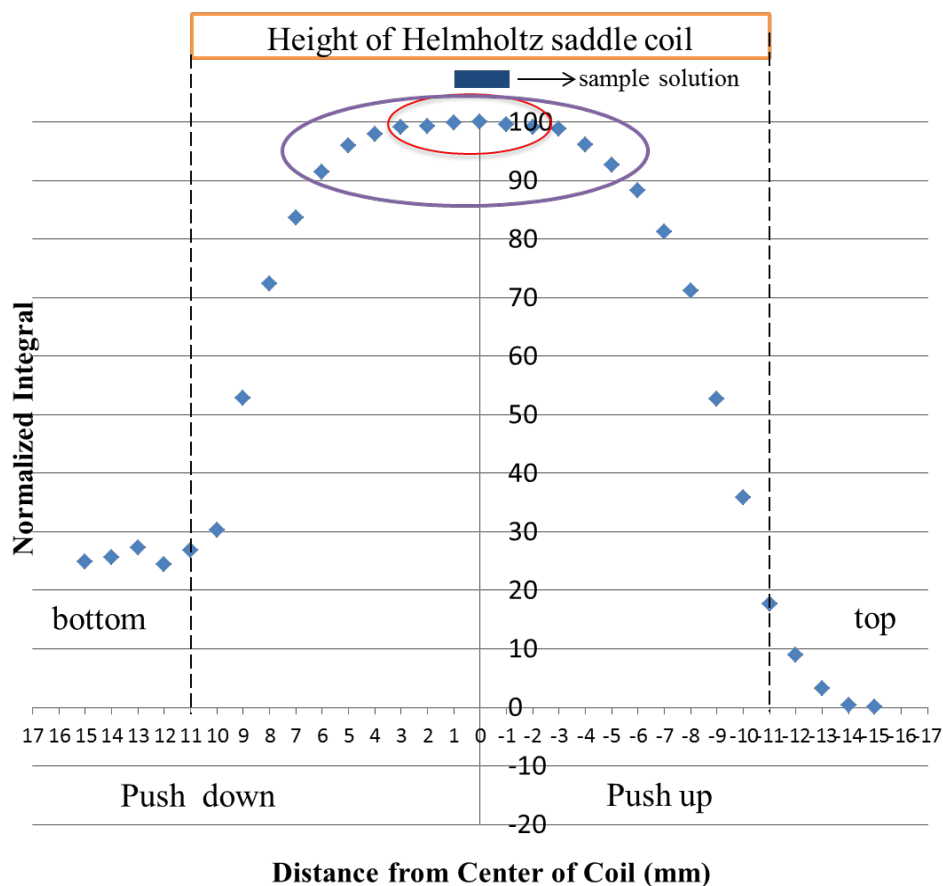


Figure 2.14. Normalized integration values of the ethanol CH<sub>3</sub>-group in a 2-mm cylindrical sample height as a function of sample position, where the origin (distance = 0 mm) indicates the center of the Helmholtz saddle coils.

When the solution is diluted by a factor of 20, the SNR of the CH<sub>3</sub> group will change to 6.5:1. Even though this is a low value, an NMR signal at this SNR is still sufficient to be observed and used for qNMR.

After the dilution by a factor of 20, the number of ethanol molecules that remain in the 6-mm sample area is  $1.07 \times 10^{17}$  ( $= 2.15 \times 10^{18} / 20$ ). An increased number of scans in an NMR experiment lead to a SNR that increases by the square root of the number of scans.

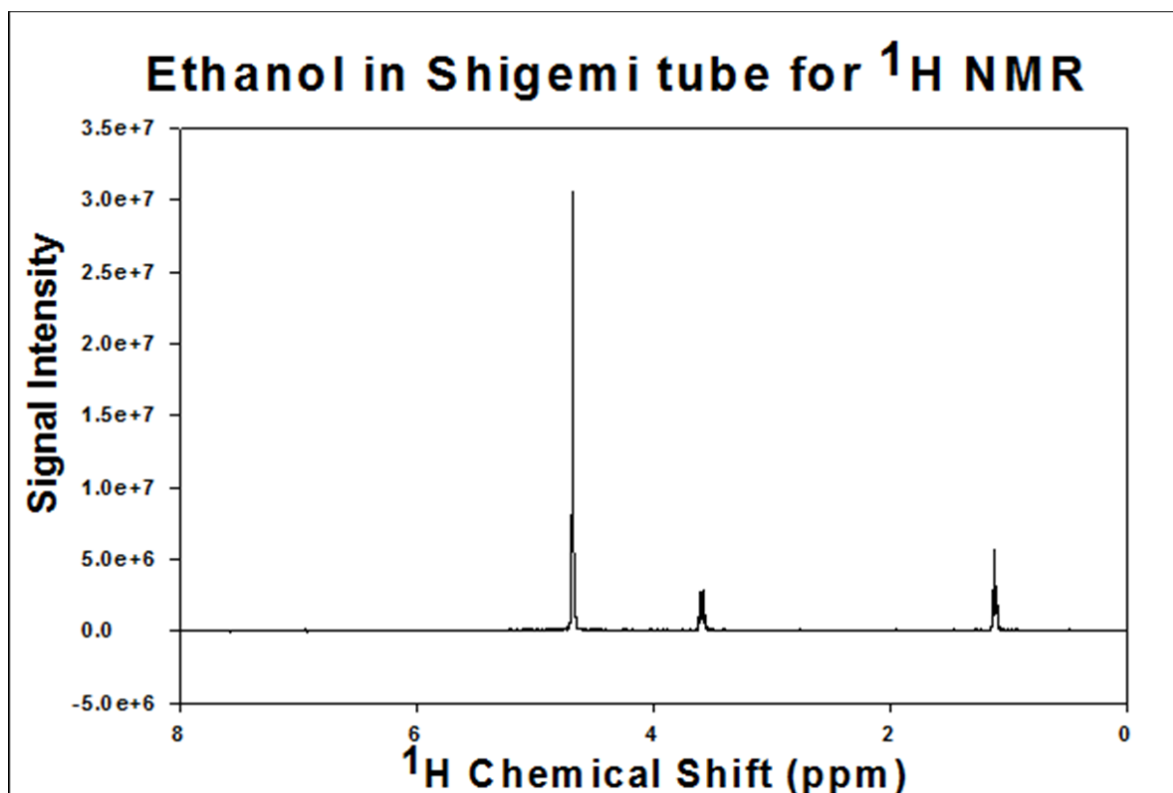


Figure 2.15.  $^1\text{H}$  NMR spectrum obtained from a single-scan experiment of 0.1086 mL from a solution of 0.40 mg ethanol in 833.0 mg  $\text{D}_2\text{O}$  in a Shigemi tube. The SNR was determined at 130:1.

For example, when the number of scan is increased from 1 to 64, the SNR will increase by a factor of 8 (i.e., from 6.5:1 to 52:1). However, there is a trade-off between the number of scans and the time it takes to run an NMR experiment. For fast-changing pH values, 64 scans (which take about 5 min to run the experiment) was found reasonable for most NMR-pH studies. Conducting a 64-scan experiment makes it possible to reduce the number of molecules that lead to a reasonable SNR in the NMR spectrum by another factor of 8; accordingly the number of molecules can be reduced to  $1.34 \times 10^{16}$  ( $= 1.07 \times 10^{17} / 8$ ). Because the  $\text{CH}_3$  group of ethanol contains three  $^1\text{H}$  nuclei, the number of nuclei contributing to the NMR signal in the 6-mm coil volume is actually

$4.02 \times 10^{16}$  ( $= 3 \cdot 1.34 \times 10^{16}$ ). Hence,  $4.02 \times 10^{16}$  is the minimum number of protons (or: fluorine atoms) in the strong and homogeneous  $B_1$  field of a 400-MHz NMR magnet to be observed and used for pH measurements.

### 3. MATERIALS AND METHODS

#### 3.1. MATERIALS

##### 3.1.1. pH Micro-sensor Compound Based on Changes in NMR Signal Intensity.

Phenolphthalein, 3,3-Bis(4-hydroxyphenyl)-isobenzofuran- 1(3H)-one (99.9%,Sigma-Aldrich, St. Louis, MO, USA) can be used as NMR pH micro-sensor compound in aqueous solution. The signal intensities of all aromatic protons change in the range of pH = 11.1 to 12.7, which renders the phenolphthalein system a primary paradigm for *in situ* monitoring of pH by NMR spectroscopy with the advantage of a spectral pH imprimatur. Figure 3.1 shows the two structures of phenolphthalein that are in an equilibrium that shifts with the sample pH. Within the range of pH = 11.1 to 12.7, the peak integrals of the left structure in Figure 3.1 decreases with increasing pH, while the peak integrals of the right structure increases. Outside this range, only one of the two types of phenolphthalein exists in sufficient concentration, and only the signals of this one structures is observed. For comparison and calibration, the pH of the solution was independently measured by using a pH electrode. The integral ratio of the peaks from the two structures were determined and correlated to the values measured with the pH electrode.

**3.1.2. pH Micro-sensor Compound Based on NMR Chemical Shifts.** Sodium fluoride (NaF) was used as the NMR micro-sensor compound to measure the pH of solutions based on chemical shifts. The  $^{19}\text{F}$  chemical shift of the  $\text{F}^-$  ion in sodium fluoride solution changes with pH in two separate ranges, i.e., from pH = 1.0 to 4.0 and again from pH = 11.0 to 14.0. Thus, the NaF solution system provides the paradigm of a spectral pH imprimatur for *in situ* monitoring of pH by  $^{19}\text{F}$  NMR spectroscopy.

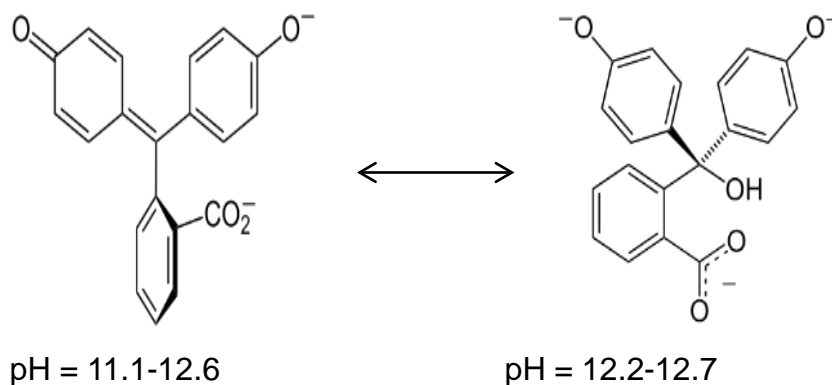


Figure 3.1. Structural difference of the pH indicator phenolphthalein depending on the pH (ref.).

### 3.2. INSTRUMENTATION, KEY PARAMETERS, AND PROCEDURES

In our experiments, NMR data were acquired from two different NMR spectrometers, a Bruker Avance III 400-MHz spectrometer using a 5-mm inverse broadband probe with  $z$ -axis gradient and a Varian INOVA 400-MHz spectrometer using a standard 5-mm broadband probe with  $z$ -axis gradient. The experiments were conducted using a predefined  $90^\circ$  pulse program (parameter: pulprog = zg) without sample spinning. A relaxation delay of  $d_1 = 5$  s was used for the *in situ* NMR pH measurements, while a delay of  $d_1 = 15$  s was used for the qNMR measurements. The *in situ* NMR pH measurements were acquired with 4 scans while the qNMR experiments were conducted with 16 scans. No automatic phasing and signal integration routines were used for the experiments conducted here because the current spectrometer software did not achieve satisfactorily phased spectra with flat baselines. The following sequence of data manipulations provided consistent results with high reproducibility and accuracy.



**3.2.1. NMR Signal Acquisition and Data Processing.** A conventional Fast Fourier transformation (FFT) of the recorded free induction decay (FID) data was conducted. The line broadening (parameter: lb) was set to an exponential, matched line-broadening value of lb = 0.3 Hz and a 1:1 zero filling of the FID data was applied; an automatic phase correction (procedure: apk) of the spectral data was performed and, if necessary, an additional manual phase correction was conducted based on the intensity of the  $^{13}\text{C}$  satellite signals; the signal integral was calculated by the integration procedure of the spectrometer software; if needed, subsequent corrections to the integral were performed interactively through the BIAS and SLOPE functions until flat integration lines were obtained to the right and to the left of the NMR signal.

**3.2.2. Phenolphthalein  $^1\text{H}$  Experimental Procedures.** In this series of experiments, 7.7 mg of phenolphthalein was dissolved in 600  $\mu\text{L}$  of  $\text{D}_2\text{O}$  (99.8% D) and an NMR spectrum was recorded. Thereafter, 3  $\mu\text{L}$  of a 0.01 M NaOH solution in  $\text{D}_2\text{O}$  was added and another NMR spectrum recorded. This procedure was repeated until a total of 30  $\mu\text{L}$  of the 0.01 M NaOH solution was added. The spectra of the phenolphthalein sample solutions at different pH values were recorded with the Varian 400-MHz high-field NMR spectrometer. NMR peaks of phenolphthalein were integrated and compared with each other. For independent calibration, the pH values of the different solutions were also measured with an electronic pH meter. The pH values from the electronic pH meter were correlated with the  $^1\text{H}$  phenolphthalein peak integrals of the *in situ* NMR pH measurements.

**3.2.3. Sodium Fluoride  $^{19}\text{F}$  Experimental Procedures.** In the  $^{19}\text{F}$  experiments, the Bruker 400-MHz high-field NMR spectrometer was used to record NMR spectra of

NaF sample solutions at different pH values. The chemical shifts of the  $F^-$  peaks at various pH values were calibrated with standard measurements of the same solutions with an electronic pH meter. As shown in Fig. 2.3. and mentioned in Chapter 2, the *in situ* NaF NMR measurements also included temperature-sensing molecules and a standard external reference solution. Thus, in this series of experiments the actual temperature was also determined by NMR.

## 4. RESULTS

### 4.1. *IN SITU* PH MEASUREMENTS IN $^1\text{H}$ NMR

The well-known pH indicator molecule Phenolphthalein, i.e., 3,3-Bis(4-hydroxy-phenyl)-isobenzofuran-1(3H)-one, can also be used as an indicator to determine the pH of a sample solution based on the change in NMR signal intensities. The  $^1\text{H}$  signal intensities of phenolphthalein change as the phenolphthalein equilibrium changes from the OH-depleted structure to the OH-rich structure (Fig. 4.1) in the range from pH = 11.1 to pH = 12.7. The resonances for the OH-depleted structure are marked by the four red boxes while the five blue boxes indicate the NMR peaks of phenolphthalein in the OH-rich form. Only one box (purple box) applies to both structures; however, the signal in this box changes from a doublet to a triplet as the structure adds the OH-group. At values below pH = 11.1, only signals from the OH-depleted form are recorded, while at values above pH = 12.7, only signals from the OH-rich form are obtained. Between pH = 11.1 and pH = 12.7, the  $^1\text{H}$  signal intensities of both forms are visible and a precise determination of pH is possible. The varying proportions of the phenolphthalein  $^1\text{H}$  signals are shown in Figure 4.2.

From the red plots in Figure 4.2, it is evident that the signal integral of NMR peaks reaches a maximum when 6  $\mu\text{L}$  of the NaOH solution was added (pH = 12.2) to the phenolphthalein sample solution. By adding more NaOH solution, the signal integrals of the OH-depleted form of phenolphthalein decrease while the signal integrals of the OH-rich form increase. The ratio between the red and blue data points is shown as a black line, which can be used as a calibration curve to measure the pH of the solution.

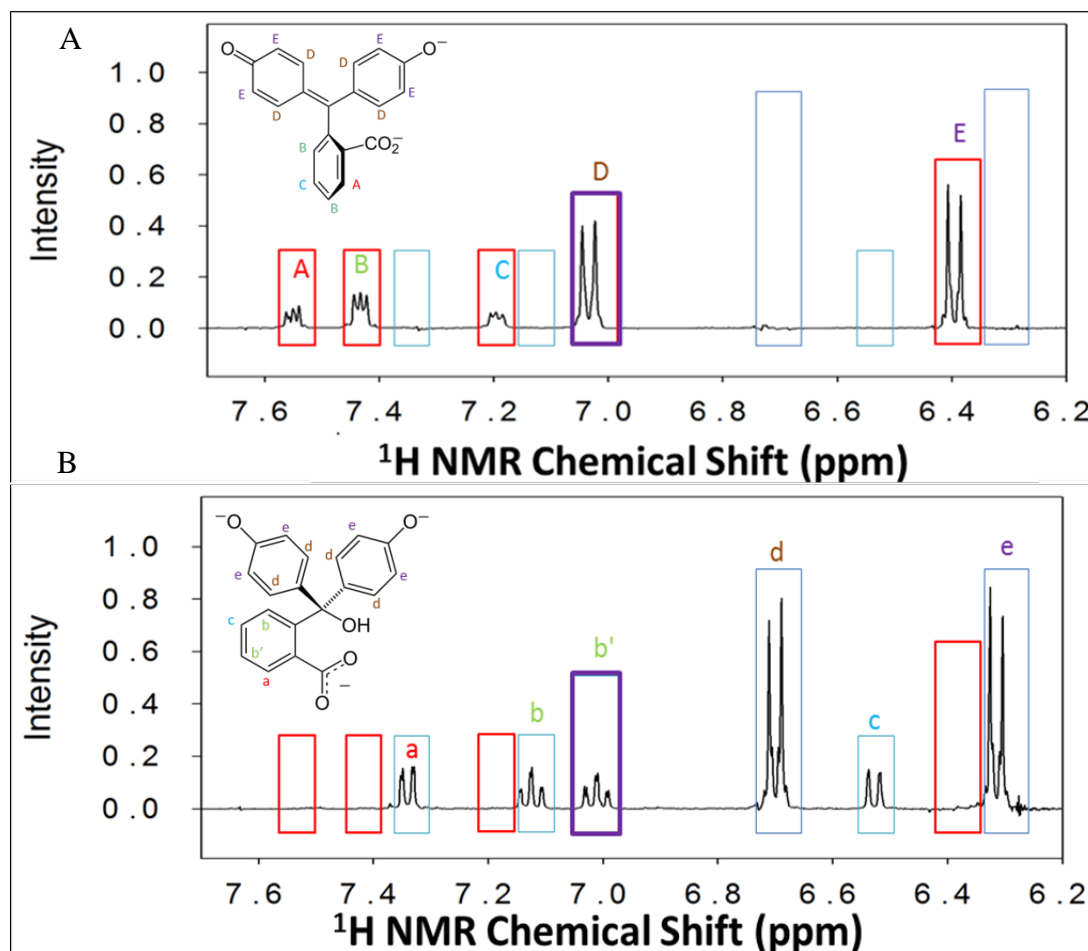


Figure 4.1.  $^1\text{H}$  NMR spectra of phenolphthalein at a) pH = 11.1. and b) pH = 12.7. Included are the two structures of phenolphthalein that are in varying equilibrium at different pH values.

#### 4.2. *IN SITU* PH MEASUREMENTS IN $^{19}\text{F}$ NMR

Aqueous sodium fluoride can be used as an indicator to measure the pH of an NMR sample solution based on chemical shifts in  $^{19}\text{F}$  NMR spectra. The  $\text{F}^-$  ion acts as the conjugated base of hydrogen fluoride (HF) and shows a very large dependency on the sample pH. With increasing pH, the equilibrium of  $\text{H}_2\text{O} + \text{F}^- \rightleftharpoons \text{HF} + \text{OH}^-$  shifts more toward the right side of the chemical equation, and the NMR signal shifts to less negative

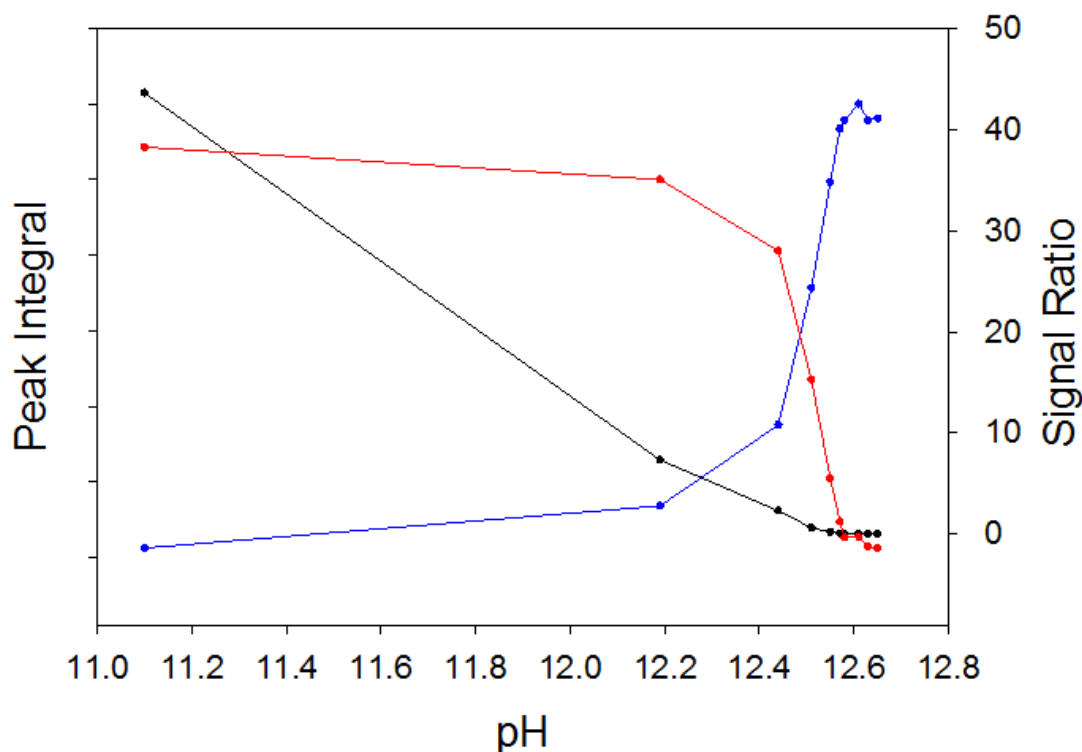


Figure 4.2. Integrated  $^1\text{H}$  NMR signal intensities of the OH-depleted (red data points) and OH-rich form (blue data points) of phenolphthalein as a function of pH. The black curve indicates the average ratio between red and blue data points.

ppm values, i.e., to the left of the  $^{19}\text{F}$  spectrum (Fig. 4.3). A similar effect is observed in the  $^1\text{H}$  NMR spectrum, where the water signal shifts with increasing pH toward higher ppm values (i.e., to the left of the spectrum). In both cases, the  $^{19}\text{F}$  and  $^1\text{H}$  nuclei, respectively, become less electron shielded because. Figure 4.3 shows  $^{19}\text{F}$  chemical shift differences in ppm of the  $\text{F}^-$  ion as a function of pH. The pH values were measured independently by an electronic pH meter. For predictive purposes, a numerical 4-parameter Chapman sigmoidal curve fit was conducted, and the equation

$$\delta = -160.4458 \text{ ppm} + 39.9351 \text{ ppm} \times (1 - \exp(-3.4439 \text{ pH}))^{1695.74} \quad (5)$$

was found to best fit the experimental data in the acidic range from pH = 1 to pH = 4. A standard 4-parameter sigmoidal curve fit according to the equation

$$\delta = -118.8817 \text{ ppm} + \frac{20.5341 \text{ ppm}}{\left(1 + \exp\left(\frac{14.5302 - \text{pH}}{0.4292}\right)\right)} \quad (6)$$

was found to best fit the experimental data in the basic range pH = 11 to pH = 14.

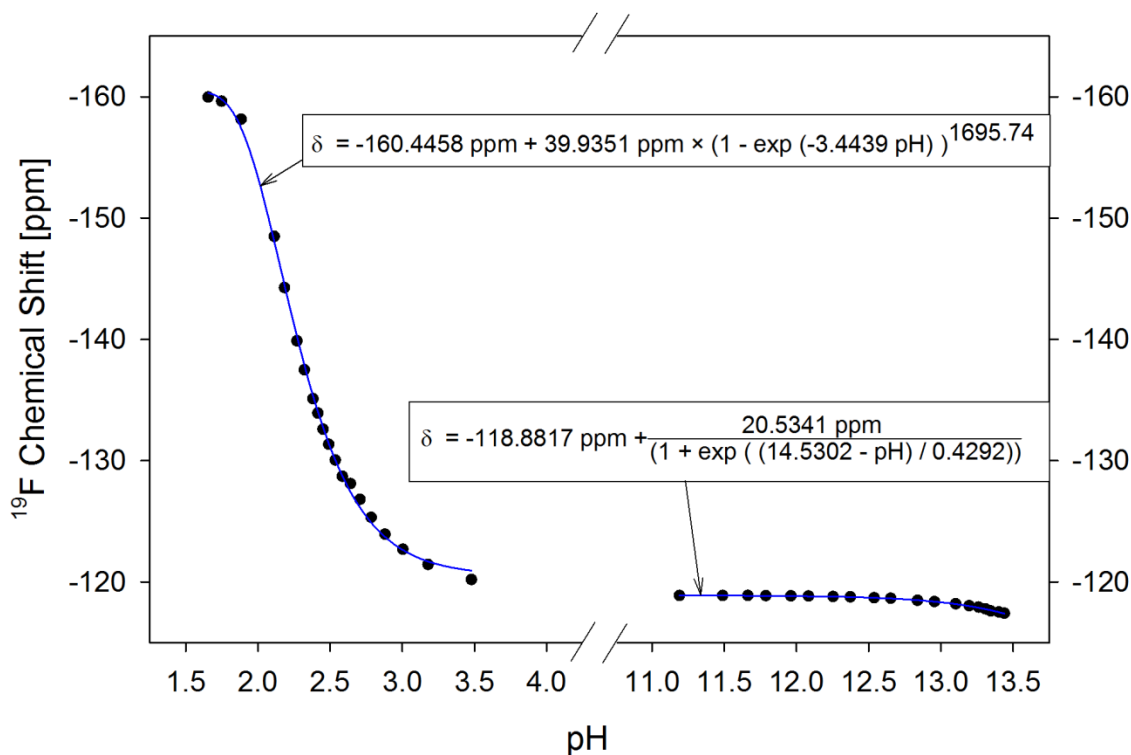


Figure 4.3.  $^{19}\text{F}$  chemical shift (ppm) of the pH micro-sensor compound NaF in aqueous solution as a function of pH.

Figure 4.4 shows NMR spectra of two compounds, pentafluorododecan-3-ol and NaF, in aqueous solution. Both molecules can be used as pH micro-sensor compound; however, while NaF is chemical-shift sensitive with respect to pH, the  $^{19}\text{F}$  signals of pentafluorododecan-3-ol show intensity dependence. A series of NMR experiments was

conducted to determine the chemical shift of the  $^{19}\text{F}$  signal of NaF at different pH values from acidic to basic. The solution was prepared from 7.0 mg of NaF and 7.7 mg of pentafluorododecan-3-ol dissolved in 600  $\mu\text{L}$  of  $\text{D}_2\text{O}$  (99.8% D). After recording the  $^{19}\text{F}$  NMR spectrum, 2.5  $\mu\text{L}$  of 0.1 M hydrochloric acid (HCl) was added changing the pH from 10.00 (original solution) to 3.48. Another  $^{19}\text{F}$  NMR spectrum was recorded and

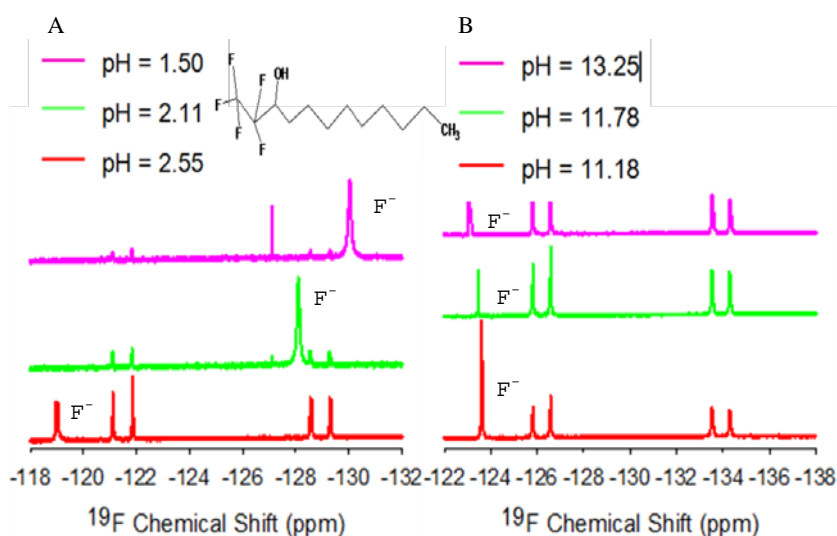


Figure 4.4  $^{19}\text{F}$  NMR spectra of pentafluorododecan-3-ol and micro-sensor compound NaF in aqueous solution at two ranges of pH (acidic and basic).

again 2.5  $\mu\text{L}$  of 0.1 M HCl added. This time, the pH value changed from 3.48 to 3.17. This procedure was repeated 3 more times until the pH finally reached pH = 1.50. In another series of experiments 2.5  $\mu\text{L}$  of 0.5 M NaOH was added so that the pH changed from 10.00 (original solution) to 11.19. Again, a  $^{19}\text{F}$  NMR spectrum was recorded and further 2.5  $\mu\text{L}$  of 0.5 M NaOH added, changing the pH from 11.19 to 11.49. The procedure was repeated 3 more times with recording NMR spectra after each step. The final pH value reached pH = 13.25. Figure 4.4(a) shows three of the NMR spectra

recorded at different pH values for the acidic solution (pH = 1.50, 2.11, 2.50). The  $^{19}\text{F}$  signal of NaF shifts dramatically to the right when the solution becomes more acidic. Figure 4.4 (b) shows three NMR spectra in basic solution (pH = 11.18, 11.78, 13.25). Here, the  $^{19}\text{F}$  signal of NaF shifts less dramatically to the left as the solution becomes more basic. The chemical shifts of the other compound, pentafluorododecan-3-ol, remain constant in both basic and acidic solutions. However, the signal intensity changes significantly with pH, so that it may also be used as  $^{19}\text{F}$  micro-sensor compound to determine the pH values in sample solutions.

The drastic change in the chemical shift of the NaF signal allows a very precise determination of the solution pH. It is estimated from the spectra in Figure 4.5 that the NaF signal shifts by 20 ppm for a pH difference of  $\Delta\text{pH} = 1$ . Because the resolution in  $^{19}\text{F}$  spectra is at least 0.2 ppm, a pH resolution of at least  $\Delta\text{pH} = 0.01$  can be predicted in this range.

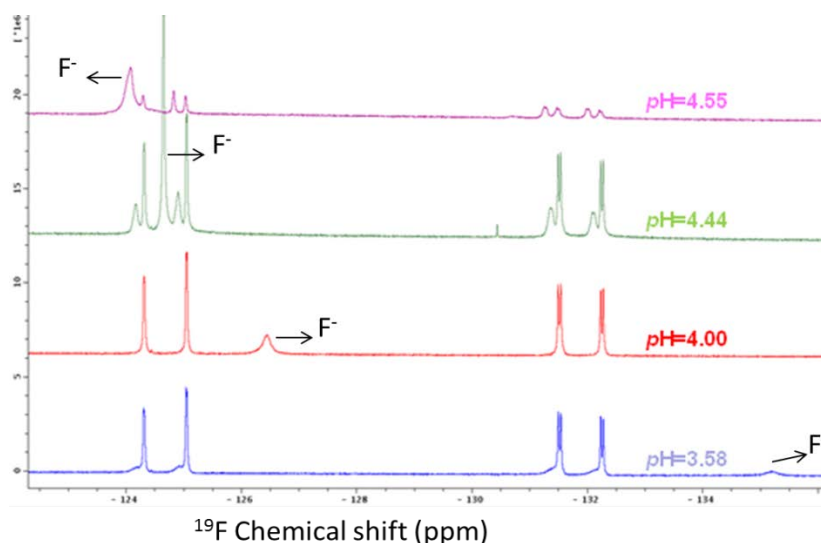


Figure 4.5.  $^{19}\text{F}$  NMR spectra of the pH micro-sensor compound NaF in the presence of pentafluorododecan-3-ol over the pH range from 3.58 to 4.55.



### 4.3. TEMPERATURE-DEPENDENT ADJUSTMENTS FOR $^{19}\text{F}$ NMR pH MEASUREMENTS

To accurately determine the pH of a sample solution with NMR spectroscopy, it is important to consider the temperature dependence of the chemical shift of  $^1\text{H}$  and  $^{19}\text{F}$  NMR signals (Section 2.1.1). It is advisable to measure the temperature together with the pH in an NMR experiment. As mentioned earlier (Section 2.1.2), ethylene glycol or methanol are appropriate temperature micro-sensor NMR compounds, which should be added to the sample solution for *in situ* temperature determination.

Figure 4.6 shows experimentally derived changes in the chemical-shift difference between the  $^{19}\text{F}$  NMR signals of NaF and trifluoroacetic acid ( $\text{CF}_3\text{COOH}$ ), i.e., in the variable  $\Delta(\Delta\delta)$ . Room temperature (298 K) was set as the reference point for this calibration, i.e.,  $\Delta(\Delta\delta)_{298\text{ K}} = 0$  ppm. As reported in Section 2.1.1, the  $^{19}\text{F}$  signal of trifluoroacetic acid shows very little temperature dependence and therefore was chosen as a temperature-independent standard for  $^{19}\text{F}$  NMR measurements.

The temperature-dependent change in the chemical shift difference between the NaF and trifluoroacetic acid signals follows a linear equation given by

$$\Delta(\Delta\delta) = -16.67 \text{ ppm} + 0.0556 T \left( \frac{\text{ppm}}{\text{K}} \right) \quad (7)$$

which is valid for the temperature range from 300 K to 330 K. Equation (7) can be used to adjust for temperature-dependent chemical-shift changes. Accurate pH determinations are therefore conducted by subtracting  $\Delta(\Delta\delta)$  from the experimentally determined  $^{19}\text{F}$  chemical shift of NaF.

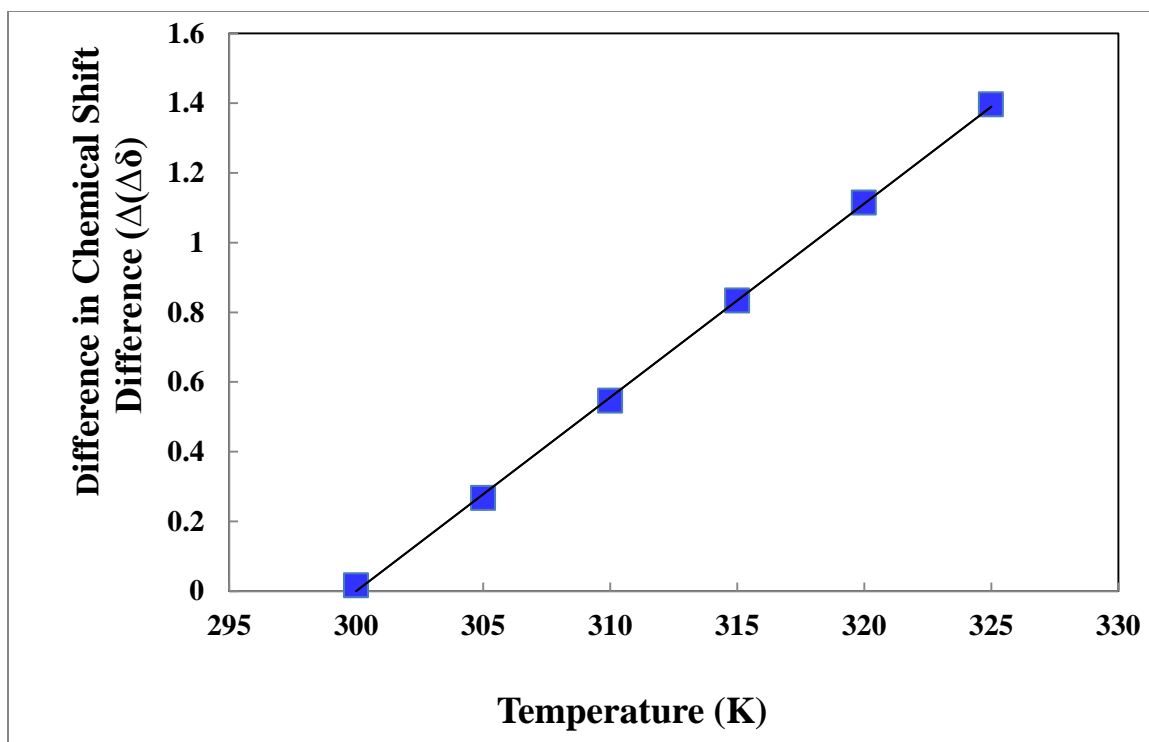


Figure 4.6. Experimentally derived changes in the chemical shift difference between the  $^{19}\text{F}$  NMR signals of NaF and trifluoroacetic acid ( $\text{CF}_3\text{COOH}$ ) at different temperatures from 300 K to 330 K.

## 5. CONCLUSION

It has been demonstrated that phenolphthalein can be used as a  $^1\text{H}$  NMR pH micro-sensor compound in the range of  $\text{pH} = 11.2$  to  $\text{pH} = 12.7$ . In this range, the signal amplitudes of phenolphthalein strongly depend on the pH of the solution. A calibration curve was established by the ratio of signal integrals from the OH-depleted form to the OH-rich form of phenolphthalein as a function of pH. The pH value was measured independently by an electronic pH meter.

It has also been demonstrated that NaF (sodium fluoride) can be used as pH micro-sensor compound in two different pH ranges (i.e.,  $\text{pH} = 1.00 - 4.00$  and  $\text{pH} = 11.00 - 14.00$ ). The chemical shift of the  $^{19}\text{F}$  NMR signals of NaF exhibit a strong dependency on the pH in these ranges, so that an accuracy of 0.01 in the pH value can easily be achieved. For example, in the 400 MHz spectrometer used in this investigation, the  $^{19}\text{F}$  chemical shift of NaF changed by more than 180 Hz when the pH was varied by only 0.01 from  $\text{pH} = 2.20$  to 2.21.

Because compounds that are added to an aqueous solution may have an influence on the pH and actually change its value, it is essential that the amount of NMR micro-sensor compound added to the sample solution is minimized. Several quantitative NMR (qNMR) experiments were conducted to determine the minimum amount of micro-sensor compound that can be used for an *in situ* NMR pH experiment. For the qNMR experiments, three types of specialized NMR tubes were chosen. Spherical NMR tubes confine the entire NMR sample to a small spherical volume that can be placed in different areas along the magnetic  $z$  axis inside the NMR probe. They can be used to determine the inner, strongest, and most homogeneous portion of the RF coil's  $B_1$  field.

Similar measurements can be achieved with Doty susceptibility plugs or Shigemi tubes. The Shigemi tubes were found to show the best performance with respect to resolution and signal-to-noise ratio (S/N). The  $B_1$  field strength along the magnetic  $z$  axis was measured by the absolute signal intensity of the  $\text{CH}_3$ -group signal of ethanol in deuterated water ( $\text{D}_2\text{O}$ ). A range of 6 mm length along the magnetic  $z$  axis in the center of coil was found to fall within 99% of the strongest  $B_1$  field. By reducing the concentration of the sample solution and by additional stoichiometric calculations, a minimum number of  $4.02 \times 10^{16}$  nuclei ( $^1\text{H}$  or  $^{19}\text{F}$ ) was found sufficient to observe NMR signals in a 400-MHz NMR spectrometer.

A new *in situ* NMR pH measuring device was developed consisting of a 5-mm NMR tube filled with the NMR sample solution and the pH micro-sensor compound. A 250- $\mu\text{m}$  i.d. capillary tube filled with trifluoroacetic acid as chemical-shift reference and a 75- $\mu\text{m}$  i.d. capillary tube filled with ethylene glycol or methanol as temperature-sensing compound were inserted into a 1-mm NMR tube, which was then placed into the center of the 5-mm NMR tube and held concentrically in place by small Teflon plugs. Using the calculated minimum number of nuclei needed for the *in situ* pH micro-sensor compound, a  $^{19}\text{F}$  NMR signal of NaF was observed in five-minute experiments with only 64 scans.

For most accurate pH measurements with the new measuring device, it is essential to know the temperature of the sample as well as the temperature dependence of the chemical shifts of the pH-sensing NMR signals. Several temperature-dependent NMR experiments were conducted and used to establish calibration curves, through which an influence of temperature on the chemical shift can be corrected. After correction it can be assumed that the chemical-shift differences are based only on variations in the pH. For

$^{19}\text{F}$  NMR spectroscopy, the signal of the trifluoroacetic acid  $\text{CF}_3$  group was found to have the least temperature-dependent chemical-shift variations. This quality renders it a superior, independent standard for temperature correction curves. Because the pH micro-sensor compound for  $^1\text{H}$  NMR spectroscopy (phenolphthalein) is based on signal-intensity changes rather than changes in the chemical shift, an independent temperature-sensing compound may not be as necessary to correct for temperature-based chemical-shift variations. However, the largely temperature independent  $^1\text{H}$  signal of the  $\text{CH}_2$  group of ethylene glycol may be used as standard in  $^1\text{H}$  NMR spectroscopy.

## BIBLIOGRAPHY

- [1] G. Orgován and B. Noszál, "Electrodeless, accurate pH determination in highly basic media using a new set of  $^1\text{H}$  NMR pH indicators," *Journal of pharmaceutical and biomedical analysis*, vol. 54, pp. 958-964, 2011.
- [2] A. Djurdjevic-Pahl, C. Hewage, and J. P. G. Malthouse, " $^{13}\text{C}$ -NMR study of the inhibition of  $\delta$ -chymotrypsin by a tripeptide-glyoxal inhibitor," *Biochemical Journal*, vol. 362, pp. 339-347, 2002.
- [3] C. Gerardin, M. In, L. Allouche, M. Haouas, and F. Taulelle, "*In situ* pH probing of hydrothermal solutions by NMR," *Chemistry of materials*, vol. 11, pp. 1285-1292, 1999.
- [4] S. Mori, S. M. Eleff, U. Pilatus, N. Mori, and P. van Zijl, "Proton NMR spectroscopy of solvent-saturable resonances: A new approach to study pH effects *in situ*," *Magnetic resonance in medicine*, vol. 40, pp. 36-42, 1998.
- [5] F. Taulelle, M. Haouas, C. Gerardin, C. Estournes, T. Loiseau, and G. Ferey, "NMR of microporous compounds: from *in situ* reactions to solid paving," *Colloids and Surfaces A: Physicochemical and Engineering Aspects*, vol. 158, pp. 299-311, 1999.
- [6] Ø. B. Vistad, D. E. Akporiaye, F. Taulelle, and K. P. Lillerud, "Morpholine, an *in situ*  $^{13}\text{C}$  NMR pH meter for hydrothermal crystallogeneses of SAPO-34," *Chemistry of materials*, vol. 15, pp. 1650-1654, 2003.
- [7] A. S. Ojugo, P. M. McSheehy, D. J. McIntyre, C. McCoy, M. Stubbs, M. O. Leach, *et al.*, "Measurement of the extracellular pH of solid tumours in mice by magnetic resonance spectroscopy: a comparison of exogenous  $^{19}\text{F}$  and  $^{31}\text{P}$  probes," *NMR in Biomedicine*, vol. 12, pp. 495-504, 1999.
- [8] [http://eduterre.ens-lyon.fr/ressources/scenarioeau/annexes/ph\\_indicators.pdf](http://eduterre.ens-lyon.fr/ressources/scenarioeau/annexes/ph_indicators.pdf).
- [9] G. Facey. (2008, March 17, 2008). *University of Ottawa NMR Facility Blog*.
- [10] "Measuring pH of Concentrated Samples," Water Analysis Instruments, Thermo Fisher Scientific 2014.
- [11] D. Harvey, *pH electrodes*: Thermo Scientific, 2014.
- [12] J. A. Illingworth, "A common source of error in pH measurements," *Biochemical Journal*, vol. 195, pp. 259-262, 1981.
- [13] Y. Wei, K. F. Hsueh, and G. W. Jang, "A study of leucoemeraldine and effect of redox reactions on molecular weight of chemically prepared polyaniline," *Macromolecules*, vol. 27, pp. 518-525, 1994.

- [14] Y. Shiau, P. Fernandez, M. J. Jackson, and S. McMonagle, "Mechanisms maintaining a low-pH microclimate in the intestine," *American Journal of Physiology-Gastrointestinal and Liver Physiology*, vol. 248, pp. G608-G617, 1985.
- [15] H. Deligianni and L. T. Romankiw, "*In situ* surface pH measurement during electrolysis using a rotating pH electrode," *IBM Journal of Research and Development*, vol. 37, pp. 85-95, 1993.
- [16] M. Dillon, "Measurement of plasma renin activity by semi-micro radioimmunoassay of generated angiotensin I," *Journal of clinical pathology*, vol. 28, pp. 625-630, 1975.
- [17] T. A. Balisky and S. S. Patel, "Electrode refilling mechanism," ed: Google Patents, 2005.
- [18] P. G. Righetti and T. Caravaggio, "Isoelectric points and molecular weights of proteins: A table," *Journal of Chromatography A*, vol. 127, pp. 1-28, 1976.
- [19] D. Fortin, B. Davis, and T. Beveridge, "Role of Thiobacillus and sulfate-reducing bacteria in iron biocycling in oxic and acidic mine tailings," *FEMS Microbiology Ecology*, vol. 21, pp. 11-24, 1996.
- [20] E. Clarke and A. H. Baldwin, "Responses of wetland plants to ammonia and water level," *Ecological Engineering*, vol. 18, pp. 257-264, 2002.
- [21] K. Popov, H. Rönkkömäki, and L. H. Lajunen, "Guidelines for NMR measurements for determination of high and low pKa values (IUPAC Technical Report)," *Pure and applied chemistry*, vol. 78, pp. 663-675, 2006.
- [22] *pH Electrode Selection Handbook* vol. ISO 9001: Thermo Fisher Scientific, 2013.
- [23] N. Incooperate. (2016). *pH Electrodes for NMR Sample Tubes*.
- [24] T. H. Nguyen, T. Venugopala, S. Chen, T. Sun, K. T. Grattan, S. E. Taylor, *et al.*, "Fluorescence based fibre optic pH sensor for the pH 10–13 range suitable for corrosion monitoring in concrete structures," *Sensors and Actuators B: Chemical*, vol. 191, pp. 498-507, 2014.
- [25] R. M. B. Silverstein, G. C. Morrill, T. C. R. M. Silverstein, G. C. Bassler, and T. C. Morrill, *Spectrometric identification of organic compounds*, 1974.
- [26] O. K. Baryshnikova, T. C. Williams, and B. D. Sykes, "Internal pH indicators for biomolecular NMR," *Journal of biomolecular NMR*, vol. 41, pp. 5-7, 2008.

- [27] U. F. Röhrig and D. Sebastiani, "NMR chemical shifts of the rhodopsin chromophore in the dark state and in bathorhodopsin: A hybrid QM/MM molecular dynamics study," *The Journal of Physical Chemistry B*, vol. 112, pp. 1267-1274, 2008.
- [28] A. M. Weljie, J. Newton, P. Mercier, E. Carlson, and C. M. Slupsky, "Targeted profiling: quantitative analysis of  $^1\text{H}$  NMR metabolomics data," *Analytical chemistry*, vol. 78, pp. 4430-4442, 2006.
- [29] M. Tiainen, H. Maaheimo, M. Niemitz, P. Soininen, and R. Laatikainen, "Spectral analysis of  $^1\text{H}$  coupled  $^{13}\text{C}$  spectra of the amino acids: Adaptive spectral library of amino acid  $^{13}\text{C}$  isotopomers and positional fractional  $^{13}\text{C}$  enrichments," *Magnetic Resonance in Chemistry*, vol. 46, pp. 125-137, 2008.
- [30] J. Zhang, C. Lin, Z. Feng, and Z. Tian, "Mechanistic studies of electrodeposition for bioceramic coatings of calcium phosphates by an *in situ* pH-microsensor technique," *Journal of Electroanalytical Chemistry*, vol. 452, pp. 235-240, 1998.
- [31] Z. Szakács, G. Hägele, and R. Tyka, " $^1\text{H}/^{31}\text{P}$  NMR pH indicator series to eliminate the glass electrode in NMR spectroscopic pK<sub>a</sub> determinations," *Analytica chimica acta*, vol. 522, pp. 247-258, 2004.
- [32] S. Moret, P. J. Dyson, and G. Laurenczy, "Direct, *in situ* determination of pH and solute concentrations in formic acid dehydrogenation and CO<sub>2</sub> hydrogenation in pressurised aqueous solutions using  $^1\text{H}$  and  $^{13}\text{C}$  NMR spectroscopy," *Dalton Transactions*, vol. 42, pp. 4353-4356, 2013.
- [33] M. Ryan, T. Liu, F. W. Dahlquist, and O. H. Griffith, "A catalytic diad involved in substrate-assisted catalysis: NMR study of hydrogen bonding and dynamics at the active site of phosphatidylinositol-specific phospholipase C," *Biochemistry*, vol. 40, pp. 9743-9750, 2001.
- [34] H.-M. Kao and C. P. Grey, "Probing the Brønsted and Lewis Acidity of Zeolite HY: A  $^1\text{H}/^{27}\text{Al}$  and  $^{15}\text{N}/^{27}\text{Al}$  TRAPDOR NMR Study of Monomethylamine Adsorbed on HY," *The Journal of Physical Chemistry*, vol. 100, pp. 5105-5117, 1996.
- [35] J. V. Shanks, "*In situ* NMR systems," *Current issues in molecular biology*, vol. 3, p. 15, 2001.
- [36] C.-C. Tai, J. Pitts, J. C. Linehan, A. D. Main, P. Munshi, and P. G. Jessop, "*In situ* formation of ruthenium catalysts for the homogeneous hydrogenation of carbon dioxide," *Inorganic chemistry*, vol. 41, pp. 1606-1614, 2002.
- [37] P. Wipf and S. Ribe, "Zirconocene-zinc transmetalation and *in situ* catalytic asymmetric addition to aldehydes," *The Journal of Organic Chemistry*, vol. 63, pp. 6454-6455, 1998.



- [38] T. L. Legerton, K. Kanamori, R. L. Weiss, and J. D. Roberts, "Measurements of cytoplasmic and vacuolar pH in *Neurospora* using nitrogen-15 nuclear magnetic resonance spectroscopy," *Biochemistry*, vol. 22, pp. 899-903, 1983.
- [39] R. B. Moon and J. H. Richards, "Determination of intracellular pH by  $^{31}\text{P}$  magnetic resonance," *Journal of Biological Chemistry*, vol. 248, pp. 7276-7278, 1973.
- [40] J. K. Roberts, N. Wade-Jardetzky, and O. Jardetsky, "Intracellular pH measurements by phosphorus-31 nuclear magnetic resonance. Influence of factors other than pH on phosphorus-31 chemical shifts," *Biochemistry*, vol. 20, pp. 5389-5394, 1981.
- [41] G. Bloch, J. Chase, M. Avison, and R. Shulman, "In Vivo  $^{31}\text{P}$  NMR measurement of glucose-6-phosphate in the rat muscle after exercise," *Magnetic resonance in medicine*, vol. 30, pp. 347-350, 1993.
- [42] S. Adler, E. Shoubridge, and G. Radda, "Estimation of cellular pH gradients with  $^{31}\text{P}$ -NMR in intact rabbit renal tubular cells," *American Journal of Physiology-Cell Physiology*, vol. 247, pp. C188-C196, 1984.
- [43] A. Stevens, P. Morris, R. Iles, P. Sheldon, and J. Griffiths, "5-fluorouracil metabolism monitored in vivo by  $^{19}\text{F}$  NMR," *British journal of cancer*, vol. 50, p. 113, 1984.
- [44] C. J. Deutsch and J. S. Taylor, "Intracellular pH as Measured by  $^{19}\text{F}$  NMRa," *Annals of the New York Academy of Sciences*, vol. 508, pp. 33-47, 1987.
- [45] K. Wade, J. Troke, C. Macdonald, I. Wilson, and J. Nicholson, " $^{19}\text{F}$  NMR studies of the metabolism of trifluoromethylaniline," in *Bioanalysis of Drugs and Metabolites, Especially Anti-Inflammatory and Cardiovascular*, ed: Springer, 1988, pp. 383-388.
- [46] J. B. Gerken, "Measurement of pH by NMR spectroscopy in concentrated aqueous fluoride buffers," *Journal of fluorine chemistry*, vol. 132, pp. 68-70, 2011.
- [47] C. J. Jameson, ed. University of Illinois at Chicago: Cynthia J. Jameson.
- [48] K. Gademann, B. Jaun, D. Seebach, R. Perozzo, L. Scapozza, and G. Folkers, "Temperature-Dependent NMR and CD Spectra of  $\beta$ -Peptides: On the Thermal Stability of  $\beta$ -Peptide Helices—Is the Folding Process of  $\beta$ -Peptides Non-cooperative?," *Helvetica chimica acta*, vol. 82, pp. 1-11, 1999.
- [49] J. R. Lyerla, C. S. Yannoni, and C. A. Fyfe, "Chemical applications of variable-temperature CPMAS NMR spectroscopy in solids," *Accounts of Chemical Research*, vol. 15, pp. 208-216, 1982.

- [50] D. S. Raiford, C. L. Fisk, and E. D. Becker, "Calibration of methanol and ethylene glycol nuclear magnetic resonance thermometers," *Analytical Chemistry*, vol. 51, pp. 2050-2051, 1979.
- [51] F. D. Doty, G. Entzminger, J. Kulkarni, K. Pamarthy, and J. P. Staab, "Radio frequency coil technology for small-animal MRI," *NMR in Biomedicine*, vol. 20, pp. 304-325, 2007.
- [52] C. Simmler, J. G. Napolitano, J. B. McAlpine, S.-N. Chen, and G. F. Pauli, "Universal quantitative NMR analysis of complex natural samples," *Current opinion in biotechnology*, vol. 25, pp. 51-59, 2014.
- [53] L. Chi, "CapPack devices for enhanced qNMR measurements in  $^1\text{H}$  NMR spectroscopy," 2015.
- [54] R. Espina, L. Yu, J. Wang, Z. Tong, S. Vashishtha, R. Talaat, *et al.*, "Nuclear magnetic resonance spectroscopy as a quantitative tool to determine the concentrations of biologically produced metabolites: implications in metabolites in safety testing," *Chemical research in toxicology*, vol. 22, pp. 299-310, 2008.
- [55] G. F. Pauli, T. Godecke, B. U. Jaki, and D. C. Lankin, "Quantitative  $^1\text{H}$  NMR. Development and potential of an analytical method: an update," *Journal of natural products*, vol. 75, pp. 834-851, 2012.
- [56] X. Liu, M. X. Kolpak, J. Wu, and G. C. Leo, "Automatic analysis of quantitative NMR data of pharmaceutical compound libraries," *Analytical chemistry*, vol. 84, pp. 6914-6918, 2012.
- [57] P. A. Hays, "Proton nuclear magnetic resonance spectroscopy (NMR) methods for determining the purity of reference drug standards and illicit forensic drug seizures," *Journal of Forensic Science*, vol. 50, pp. JFS2005124-19, 2005.
- [58] P. Maes, Y. B. Monakhova, T. Kuballa, H. Reusch, and D. W. Lachenmeier, "Qualitative and quantitative control of carbonated cola beverages using  $^1\text{H}$  NMR spectroscopy," *Journal of agricultural and food chemistry*, vol. 60, pp. 2778-2784, 2012.
- [59] P. Lacy, R. T. McKay, M. Finkel, A. Karnovsky, S. Woehler, M. J. Lewis, *et al.*, "Signal intensities derived from different NMR probes and parameters contribute to variations in quantification of metabolites," *PloS one*, vol. 9, p. e85732, 2014.
- [60] S. Mahajan and I. P. Singh, "Determining and reporting purity of organic molecules: why qNMR," *Magnetic Resonance in Chemistry*, vol. 51, pp. 76-81, 2013.
- [61] Wilmad-LabGlass. *SP Scienceware*.
- [62] Wilmad-LabGlasses. *Doty Susceptibility Plugs*.

- [63] L. Network. *Doty Susceptibility Plugs*.
- [64] S. N. Incorporations. *Advanced NMR Microtubes*.
- [65] T. R. Dulski, "A manual for the chemical analysis of metals," 1996.

## VITA

Ming Huang was born in Tianjin, China. In June 2012, she obtained a bachelor's degree in Department of Environment Science and Engineering, Nankai University of Binhai College, Tianjin, R.P. China.

In August 2012, she enrolled at Missouri University of Science and Technology to pursue a Ph.D.'s degree. In July 2017, she received her master's degree in chemistry firstly under the guidance of Dr. Klaus Woelk at Missouri University of Science and Technology. Her research interest is *In situ* pH Determination Based on the NMR Analysis of  $^1\text{H}$  Signal Intensities and  $^{19}\text{F}$  Chemical Shifts, quantitative NMR.